DESIGN GUIDE FOR CALCULATING FLUID DAMPING FOR CIRCULAR CYLINDRICAL STRUCTURES

by

S. S. Chen

BASE TECHNOLOGY

ARGONNE NATIONAL LABORATORY, ARGONNE, ILLINOIS

ANL-83-54

ARGONNE NATIONAL LABORATORY
9700 South Cass Avenue
Argonne, Illinois 60439

DESIGN GUIDE FOR CALCULATING FLUID DAMPING
FOR CIRCULAR CYLINDRICAL STRUCTURES

by

S. S. Chen

Components Technology Division

June 1983

CONTENTS

5

FIGURES

TABLES

NOMENCLATURE

c	Sound velocity
[C]	Damping matrix
C_D	Drag coefficient
C_M	Added mass coefficient
C_t	Two-phase flow damping coefficient
C_v	Viscous damping coefficient
C_N	Drag coefficient for axial flow
D	Cylinder diameter
C_s	Cylinder damping coefficient
EI	Flexural rigidity of cylinder
GJ	Torsional rigidity
f_i, g_i	Total fluid force components in two orthogonal directions
f_{oi}, g_{oi}, f_o, g_o	Fluid force components that are independent of cylinder motion
f	$\omega/2\pi$
f_n	Natural frequency of nth mode (Hz)
H	Functions specified in Eqs. 6, 7, 8, and 11 for various cases
k	Fluidelastic stiffness constant
K_c	Keulegan-Carpenter parameter $(2\pi u_o/D)$
ℓ	Length of a cylinder or axial half wavelength
m	Mass per unit length of cylinder
$M_d (= \rho\pi r^2)$	Displaced mass of fluid per unit length
M_f	Added mass per unit length
N	Number of cylinders
P	Longitudinal pitch
q_i	Generalized coordinate associated with ith mode
r	Cylinder radius

R	Radius of the outside cylinder or radius of curvature for a curved tube
S	Kinetic Reynolds number $\left(\dfrac{\omega r^2}{\nu}\right)$
S_f	Forced Strouhal frequency
S_n	Strouhal frequency
t	Time
T	Transverse pitch
$u, v, w,$ u_i, v_i	Cylinder displacements
u_o	Peak cylinder displacement
U_f	Reduced flow velocity (V/fD)
V	Flow velocity
α_e	Void fraction
$\alpha, \beta, \alpha_{ij},$ $\beta_{ij}, \sigma_{ij}, \tau_{ij}$	Added mass
$\alpha', \beta', \alpha'_{ij},$ $\beta'_{ij}, \sigma'_{ij}, \tau'_{ij}$	Fluid viscous damping
$\alpha'', \beta'', \alpha''_{ij},$ $\beta''_{ij}, \sigma''_{ij}, \tau''_{ij}$	Fluidelastic stiffness
γ	r/R
μ	Fluid viscosity
ν	Kinematic viscosity of fluid
ϕ_i	Orthonormal modal function of ith mode
ρ	Fluid density for a single phase fluid
ρ_e	Effective density for a two-phase flow
ρ'	Fluid density for the higher-density fluid in a two-phase flow
ζ_n	Modal damping ratio of nth mode
ω	Oscillation frequency
ω_n	Natural frequency of nth mode in radian/second

DESIGN GUIDE FOR CALCULATING FLUID DAMPING
FOR CIRCULAR CYLINDRICAL STRUCTURES

by

S. S. Chen

ABSTRACT

Fluid damping plays an important role for structures submerged in fluid, subjected to flow, or conveying fluid. This design guide presents a summary of calculational procedures and design data for fluid damping for circular cylinders vibrating in quiescent fluid, crossflow, and parallel flow.

I. INTRODUCTION

Fluid damping is the result of energy dissipation caused by the motion of a structure relative to a fluid. It plays an important role for oscillations of structures submerged in fluid, subjected to flow, or conveying fluid. It affects structural response amplitude and stability boundaries. To understand the vibrational behavior of a structural system vibrating in a fluid, to calculate the response amplitude, and to predict the stability-instability boundary, we have to determine the magnitude of fluid damping.

Fluid damping arises from many different sources. In a quiescent viscous flow, the drag force acting on a vibrating structure can contribute to the viscous type of damping. In a compressible fluid, the energy carried away by out-going waves is an energy loss and can also be modeled as viscous damping in some parameter range. In a moving fluid, other fluid force components can be very important—forces are functions of flow velocity and may act as a damping mechanism. In a certain parameter range, the nature of this flow-velocity-dependent force may change from an energy-dissipating mechanism to a destabilizing effect and cause structural instability.

Studies of fluid damping for circular cylinders in various flow conditions have been reported. The objective of this design guide is to summarize the results, which may be useful in the analysis and design evaluation of structural components subjected to fluid flow—in particular, for applications to nuclear internal and plant components. Most of the material in the design guide is based on a recent review [1]. Specifically, this design guide includes:

Some general considerations of fluid damping,

Damping in quiescent fluids,

Damping in parallel flow,

Damping in crossflow, and

Examples of fluid damping.

II. SOME GENERAL CONSIDERATIONS

1. Fluid Force Components

Consider an array of N circular cylinders oscillating in a flow as shown in Fig. 1. The axes of the cylinders are parallel to the z axis. The subscript i is used to denote variables associated with cylinder i. The displacement components of cylinder i are u_i and v_i and fluid force components are f_i and g_i, respectively. There are several types of fluid forces [2,3]:

1. Fluid inertia force—fluid force that is proportional to the cylinder acceleration.

2. Fluid damping force—fluid force that is proportional to the cylinder velocity.

3. Fluidelastic stiffness force—fluid force that is proportional to the cylinder displacement.

4. Fluid excitation force—fluid force that is independent of the cylinder motion.
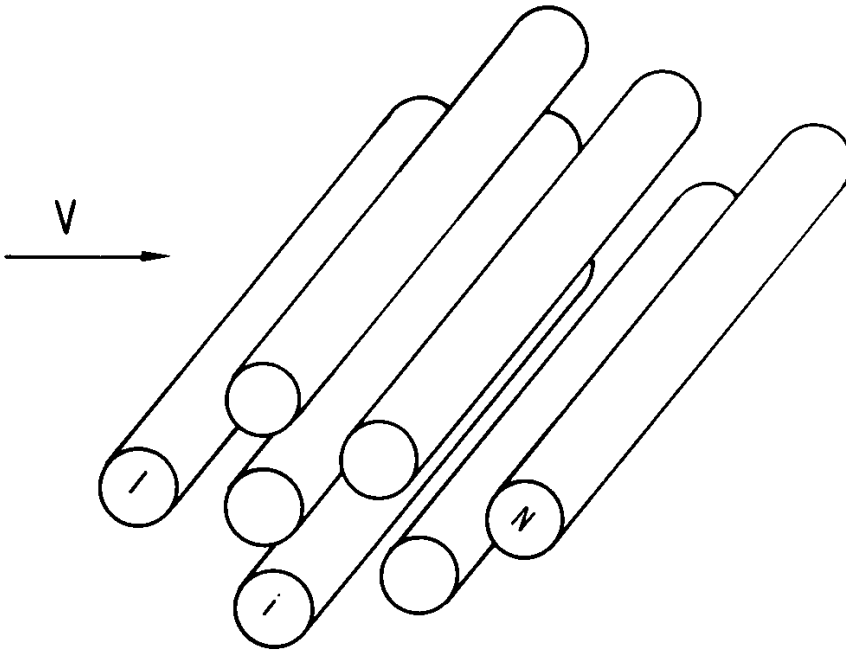
(a) A GROUP OF CIRCULAR CYLINDERS
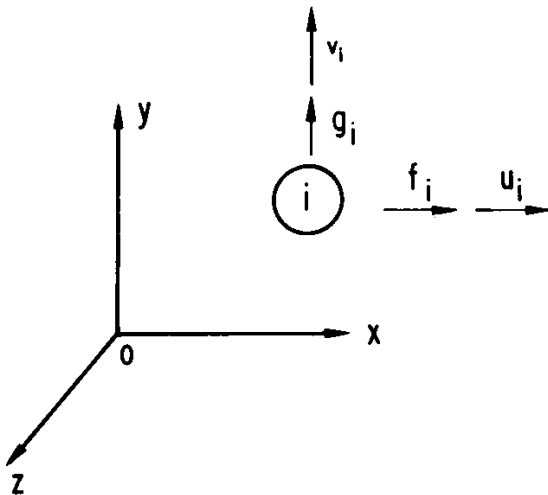
(b) FLUID FORCE AND CYLINDER DISPLACEMENT
COMPONENTS

Fig. 1. Schematic of a circular cylinder array; (a) a group of circular
cylinders; (b) fluid force and cylinder displacement components.

Mathematically, these fluid force components can be written:

$$f_i = \sum_{j=1}^{N} \left\{ \left[\alpha_{ij} \frac{\partial^2 u_j}{\partial t^2} + \alpha'_{ij} \frac{\partial u_j}{\partial t} + \alpha''_{ij} u_j \right] + \left[\sigma_{ij} \frac{\partial^2 v_j}{\partial t^2} \right. \right.$$

$$\left. \left. + \sigma'_{ij} \frac{\partial v_j}{\partial t} + \sigma''_{ij} v_j \right] \right\} + f_{oi} ,$$

and (1)

$$g_i = \sum_{j=1}^{N} \left\{ \left[\tau_{ij} \frac{\partial^2 u_j}{\partial t^2} + \tau'_{ij} \frac{\partial u_j}{\partial t} + \tau''_{ij} u_j \right] + \left[\beta_{ij} \frac{\partial^2 v_j}{\partial t^2} \right. \right.$$

$$\left. \left. + \beta'_{ij} \frac{\partial v_j}{\partial t} + \beta''_{ij} v_j \right] \right\} + g_{oi} .$$

The components in the brackets are called motion-dependent fluid forces; these components vanish if the cylinders are stationary. f_{oi} and g_{oi} are resultant fluid excitation forces that are independent of cylinder motion. Note that α_{ij}, σ_{ij}, τ_{ij}, and β_{ij} are added mass matrices; α'_{ij}, σ'_{ij}, τ'_{ij}, and β'_{ij} are damping matrices, and α''_{ij}, σ''_{ij}, τ''_{ij}, and β''_{ij} are fluidelastic stiffness matrices. In general, these matrices depend on cylinder motion, in particular, the displacement (u_i, v_i), velocity ($\partial u_i / \partial t$, $\partial v_i / \partial t$), and acceleration ($\partial^2 u_i / \partial t^2$, $\partial^2 v_i / \partial t^2$), and the flow velocity (V). However, in many practical situations, added mass matrices are independent of cylinder motion and flow velocity V, while damping and fluidelastic matrices are functions of flow velocity V only.

Equation 1 can be written as a single matrix equation:

$$\{F\} = [M]\{\ddot{q}\} + [C]\{\dot{q}\} + [K]\{q\} + \{Q\}. \tag{2}$$

For a single cylinder, the motions in the two directions are uncoupled in most cases; therefore, the two force components can be written:

$$f = \alpha \frac{\partial^2 u}{\partial t^2} + \alpha' \frac{\partial u}{\partial t} + \alpha'' u + f_o ,$$

and (3)

$$g = \beta \frac{\partial^2 v}{\partial t^2} + \beta' \frac{\partial v}{\partial t} + \beta'' v + g_o .$$

Furthermore, in some situations, the motion is independent of the direction of oscillations; i.e., either one of the components of Eq. 3 is applicable and can be written as follows:

$$f = C_M M_d \frac{\partial^2 u}{\partial t^2} + C_v \frac{\partial u}{\partial t} + ku + f_o ,
\tag{4}$$

where M_d is the displaced mass per unit length of fluid by the cylinder, C_M is the added mass factor, C_v is the viscous damping coefficient, and k is the fluidelastic stiffness constant.

2. Fluid Damping Coefficients

Without loss of generality, consider a single cylinder oscillating with a displacement given by $u = u_o \cos \omega t$ in a flow with a mean flow velocity V. In this case, the following dimensionless parameters are important:

Reynolds number $Re = \frac{VD}{\nu}$,

Reduced flow velocity $U_f = \frac{V}{fD}$,

Kinetic Reynolds number $S = \frac{\omega r^2}{\nu}$,

Keulegan-Carpenter parameter $K_c = \frac{2\pi u_o}{D}$.

The first two parameters are associated with the mean flow and the last two parameters are associated with the oscillations of the cylinder. Fluid damping matrices α'_{ij}, σ'_{ij}, τ'_{ij}, and β'_{ij} in Eqs. 1 and [C] in Eq. 2, and fluid damping coefficients α' and β' in Eqs. 3 and C_v in Eq. 4, in general, are functions of Re, U_f, S, and K_c.

In most cases, we are interested in small-amplitude oscillations; i.e., K_c is very small. Then fluid damping is a function of Re, S, and U_f only. The following two situations are of particular importance:

1.   In quiescent fluid, fluid damping is a function of S only.

2.   In flowing fluid, fluid damping is a function of U_f only.

In other situations, other approximations can be applied.

A summary of available results on damping will be presented based on Eqs. 1 to 4 for three different flow conditions: quiescent fluid, parallel flow, and crossflow.

III. QUIESCENT FLUID

For structures vibrating in a quiescent fluid, fluid damping consists of (1) fluid viscous effect and (2) energy carried away by acoustic waves. Available results are listed in the following text.

1.   A Circular Cylinder in a Concentric Annular Viscous Fluid

A circular cylinder vibrating in a confined viscous fluid, as shown in Fig. 2, was studied theoretically and experimentally by Chen et al. [4,5]. A closed-form solution for the fluid force was obtained using the linearized, two-dimensional Navier-Stokes equations of motion. Let the cylinder perform a small sinusoidal motion $u(t)(= u_0 \cos \omega t)$. The fluid force per unit length acting on the cylinder is

$$f = C_M M_d \frac{d^2 u}{dt^2} + C_v \frac{du}{dt} \,, \tag{5}$$

where

$$C_M = \mathrm{Re}(H) ,$$

$$C_v = -M_d \omega \mathrm{Im}(H) ,$$

$$
\begin{aligned}
H = & \{2a^2[I_0(a)K_0(b) - I_0(b)K_0(a)] - 4a[I_1(a)K_0(b) + I_0(b)K_1(a)] \\
& + 4a\gamma[I_0(a)K_1(b) + I_1(b)K_0(a)] - 8\gamma[I_1(a)K_1(b) - I_1(b)K_1(a)]\} \\
& \div \{a^2(1 - \gamma^2)[I_0(a)K_0(b) - I_0(b)K_0(a)] \\
& + 2a\gamma[I_0(a)K_1(b) - I_1(b)K_0(b) + I_1(b)K_0(a) - I_0(b)K_1(b)] \\
& + 2a\gamma^2[I_0(b)K_1(a) - I_0(a)K_1(a) - I_1(a)K_0(b) - I_1(a)K_0(a)]\} - 1 \,,
\end{aligned}
\tag{6}
$$

$$a = (1 + i) \sqrt{\frac{\omega r^2}{2\nu}} \,,$$
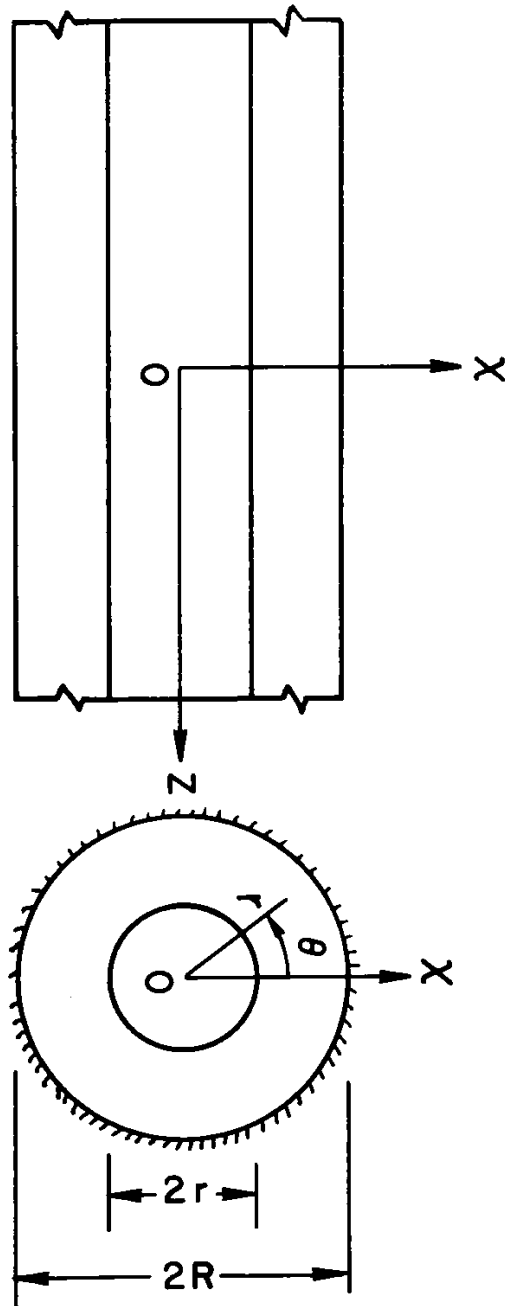
Fig. 2. Schematic and coordinate system of a cylinder vibrating in
         fluid annulus.

$$b = (1 + i) \sqrt{\frac{\omega r^2}{2\nu}} \ ,$$

$$\gamma = r/R \ , \tag{6}$$

(Contd.)

$$M_d = \rho \pi r^2 \ .$$

The values of C_M and C_v depend on H, which, in turn, is a function of the radius ratio r/R and kinetic Reynolds number S ($= \omega r^2/\nu$). The values of Re(H) and $-$Im(H) are given in Figs. 3 and 4, respectively.

When the absolute values of a and b in Eqs. 6 are large (e.g., both $|a|$ and $|b| > 50$), H can be simplified:

$$H = \frac{[a^2(1 + \gamma^2) - 8\gamma]\sinh(b - a) + 2\alpha(2 - \gamma + \gamma^2)\cosh(b - a) - 2\gamma^2\sqrt{ab} - 2a\gamma\sqrt{\gamma}}{a^2(1 - \gamma^2)\sinh(b - a) - 2a\gamma(1 + \gamma)\cosh(b - a) + 2\gamma^2(ab) + 2a\gamma\sqrt{\gamma}} \ . \tag{7}$$

As the radius ratio becomes infinite, H given in Eq. 6 becomes

$$H = 1 + \frac{4K_1(a)}{aK_0(a)} \ . \tag{8}$$

The values of H are given in Fig. 5 as a function of S($= \omega r^2/\nu$). This corresponds to the case of a circular cylinder vibrating in an infinite viscous fluid.

Based on the boundary-layer approximation, Sinyavskii et al. [6] has developed approximate expressions for C_M and C_v:

$$C_M = \frac{R^2 + r^2}{R^2 - r^2} + \frac{2}{r} \left(\frac{2\nu}{\omega}\right)^{1/2} \ ,$$

and

$$C_v = \frac{4\pi\mu r}{\sqrt{\frac{2\nu}{\omega}}} \left[\frac{R^4 + r^3R}{(R^2 - r^2)^2}\right] \ , \tag{9}$$

where $\sqrt{\omega/2\nu}$ is the viscous penetration depth. Note that Eq. 9 is similar to Eq. 7; it is applicable for $\omega r^2/\nu \gg 1$. In many practical applications, Eq. 9 can be employed.
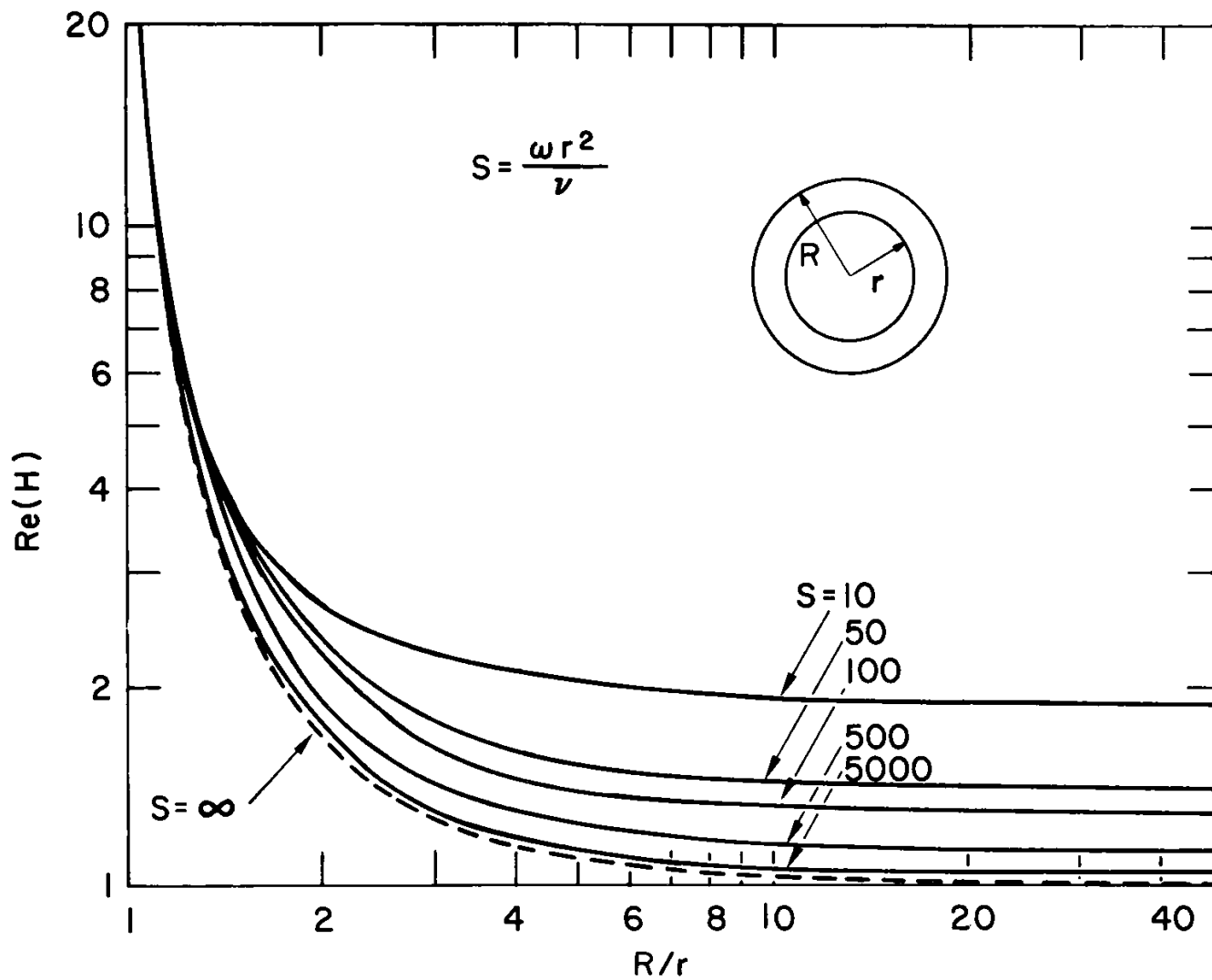
Fig. 3. Real values of H as a function of R/r for selected values of S [Ref. 4].
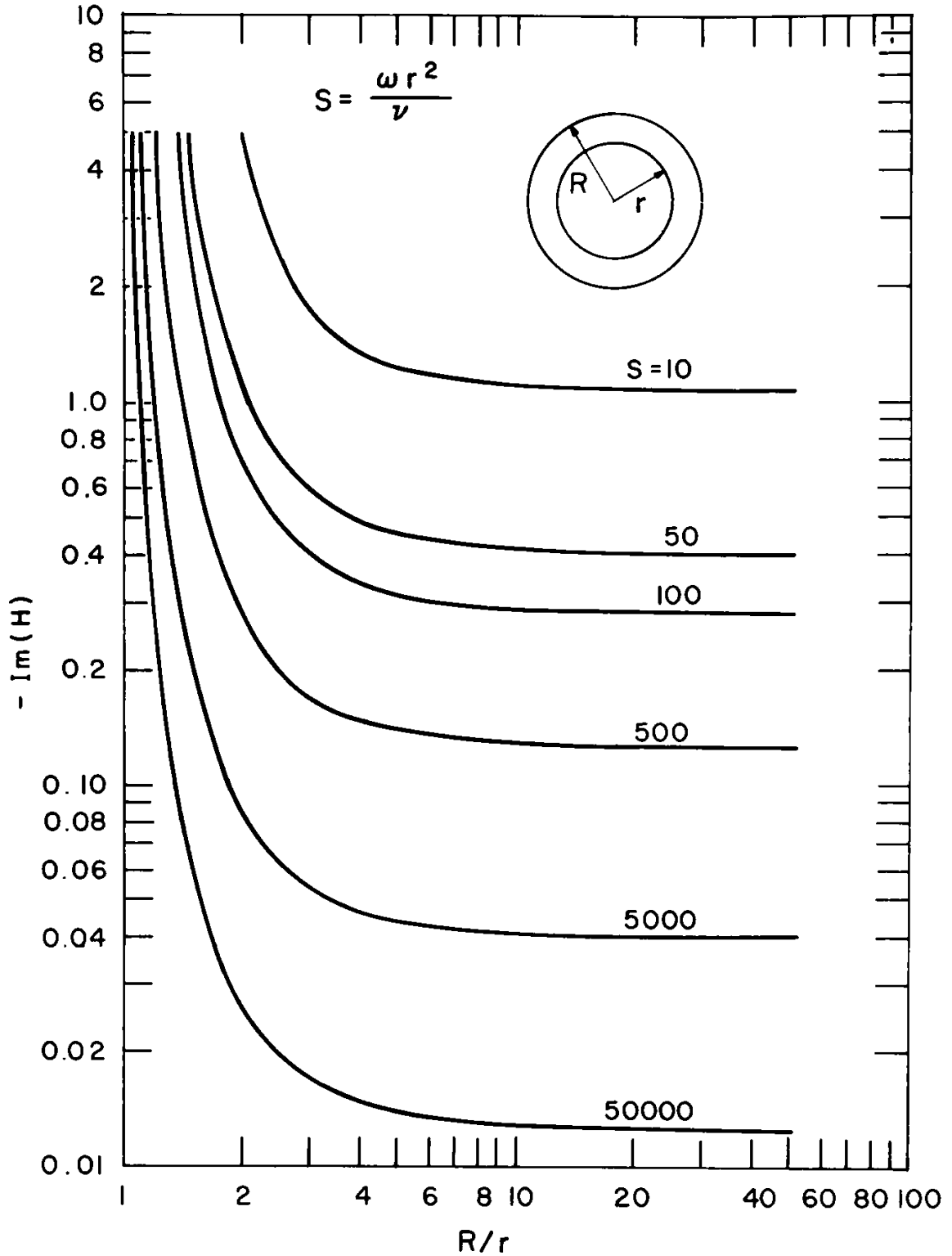
Fig. 4. Imaginary values of H as a function of R/r for selected values of S [Ref. 4].
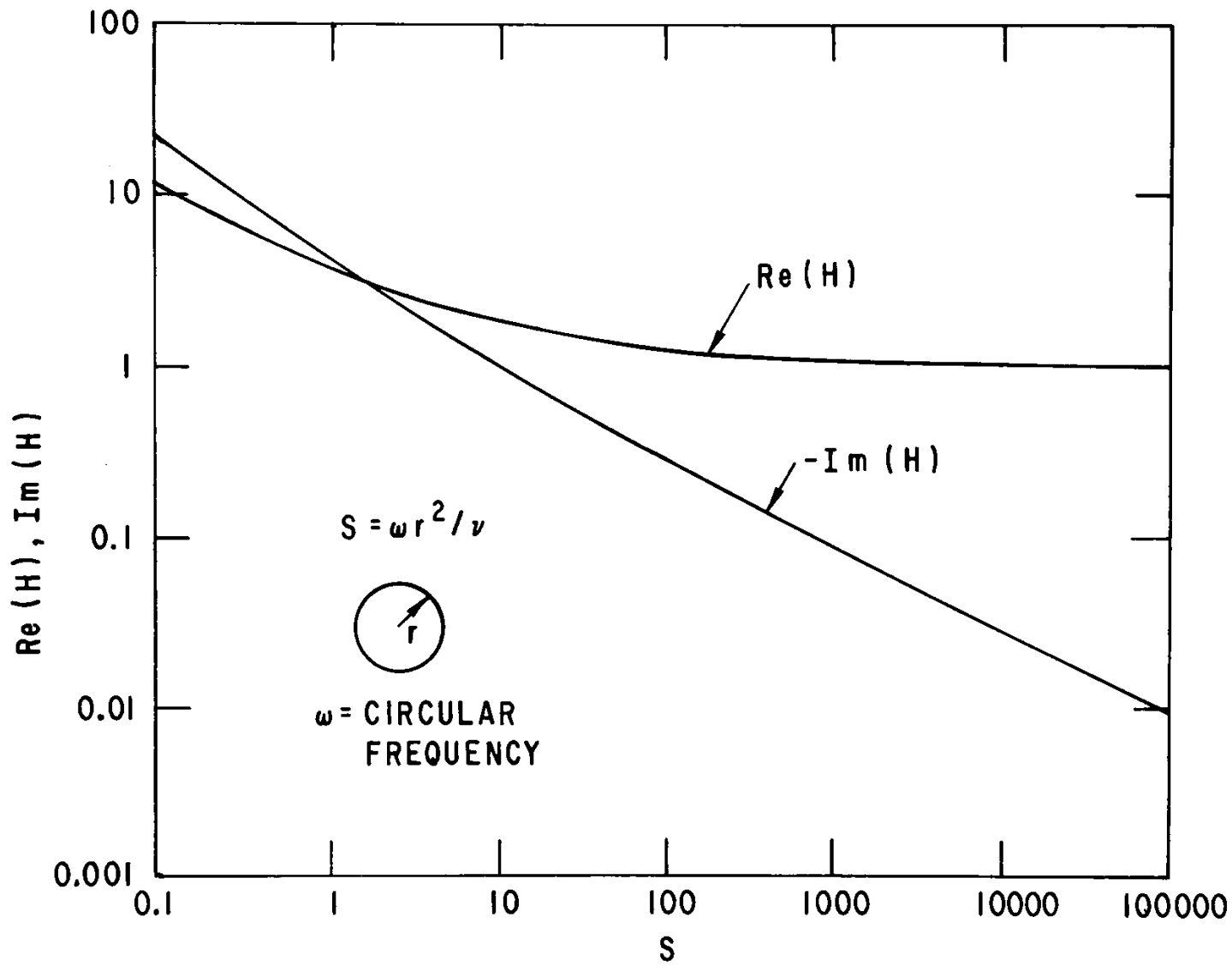
Fig. 5. Real and imaginary values of H for a cylinder vibrating in an infinite fluid.

Several additional approximate solutions for C_M and C_v also are given in Section III.5.

The theoretical results and experimental data agree well for both a cylinder oscillating in an infinite fluid [7] and in an annular region [4,6]. However, the linear theory is applicable only for small-amplitude oscillations (see Section III.10 for discussions).

For a uniform cylinder with mass per-unit length m, the modal damping ratio attributed to fluid viscosity is [4]

$$\zeta_n = -\frac{1}{2} \left(\frac{M_d}{C_M M_d + m}\right) Im(H) \ . \tag{10}$$

The analytical results for ζ_n were verified using several viscous fluids [4]; the agreement between theory and experiment is good.

2.   A Circular Cylinder in a Finite-Length Annular Viscous Region

When the length of the annular region is small (see Fig. 6; L is the same order of magnitude as r), the three-dimensional effect becomes significant. An approximate solution for this case was obtained by Mulcahy [8]. It is based on the linearized Navier-Stokes equations and the assumption that the gap clearance is much less than the cylinder radius r. The fluid force acting on the cylinder is given by

$$f = C_M M_d \frac{\partial^2 u}{\partial t^2} + C_v \frac{\partial u}{\partial t} \ ,$$

$$C_M = \left(\frac{r}{R-r}\right) Re(H) \left[1 - \frac{\cosh(z/R)}{\cosh(L/R)}\right] \ ,$$

$$C_v = -M_d \left(\frac{r}{R-r}\right) \omega Im(H) \left[1 - \frac{\cosh(z/R)}{\cosh(L/R)}\right] \ , \tag{11}$$

$$H = \frac{a \sinh a}{(2 + a \sinh a - 2 \cosh a)} \ ,$$

and

$$a = (1+i) \sqrt{\frac{\omega(R-r)^2}{2\nu}} \ .$$
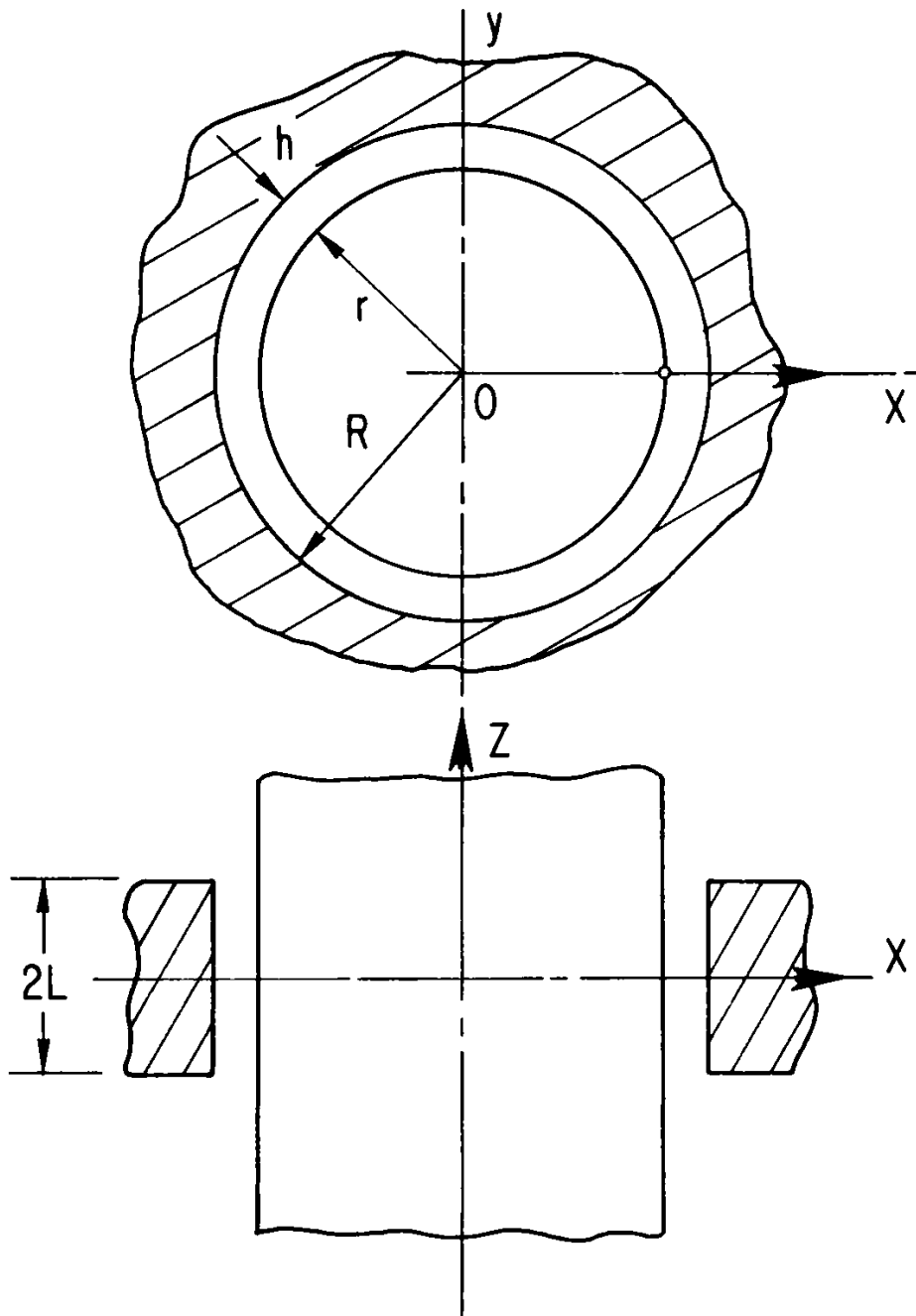
Fig. 6. A circular cylinder in fluid filled annular region.

The theoretical values of Re(H) and −Im(H) are given in Fig. 7. Experimental data are shown to agree well with the theory. The solution is valid for $(R - r)/r \ll 1$ and the viscous penetration depth $\sqrt{\omega/2\nu}$ on the order of $(R - r)$.

Note that Eq. 11 is applicable for transverse motion within the gap. The damping associated with the rotational motion is, in general, much smaller and can be ignored.

3. A Circular Cylinder in an Eccentric Annular Viscous Fluid

Closed form solution for this case is not available. However, viscous damping can be obtained using a finite-element method [9]. A system of discretized equations is obtained from the appropriate two-dimensional Navier-Stokes and continuity equations through Galerkin's process. The basic unknowns are velocity and pressure. The added mass and viscous damping coefficients are obtained through a line integration of stress and pressure around the circumference of the cylinder.

Typical results are given in Fig. 8. Both C_M and C_v increase with eccentricity.

4. A Circular Cylinder in an Infinite Compressible Inviscid Fluid

When a cylinder vibrates in a confined ideal fluid, no energy loss occurs. While in an infinite fluid, there is a radiation loss attributed to the energy carried away by the out-going waves. Let the cylinder radius be r, sound velocity in fluid c, and ocillation frequency ω. The two-dimensional solution of the fluid field yields the added mass and viscous damping coefficients [10]:

$$C_M = \frac{2\Delta_1}{a\Delta}$$

and

$$C_v = M_d \, \omega \left(\frac{2\Delta_2}{a\Delta} \right) ,$$

(12)

where
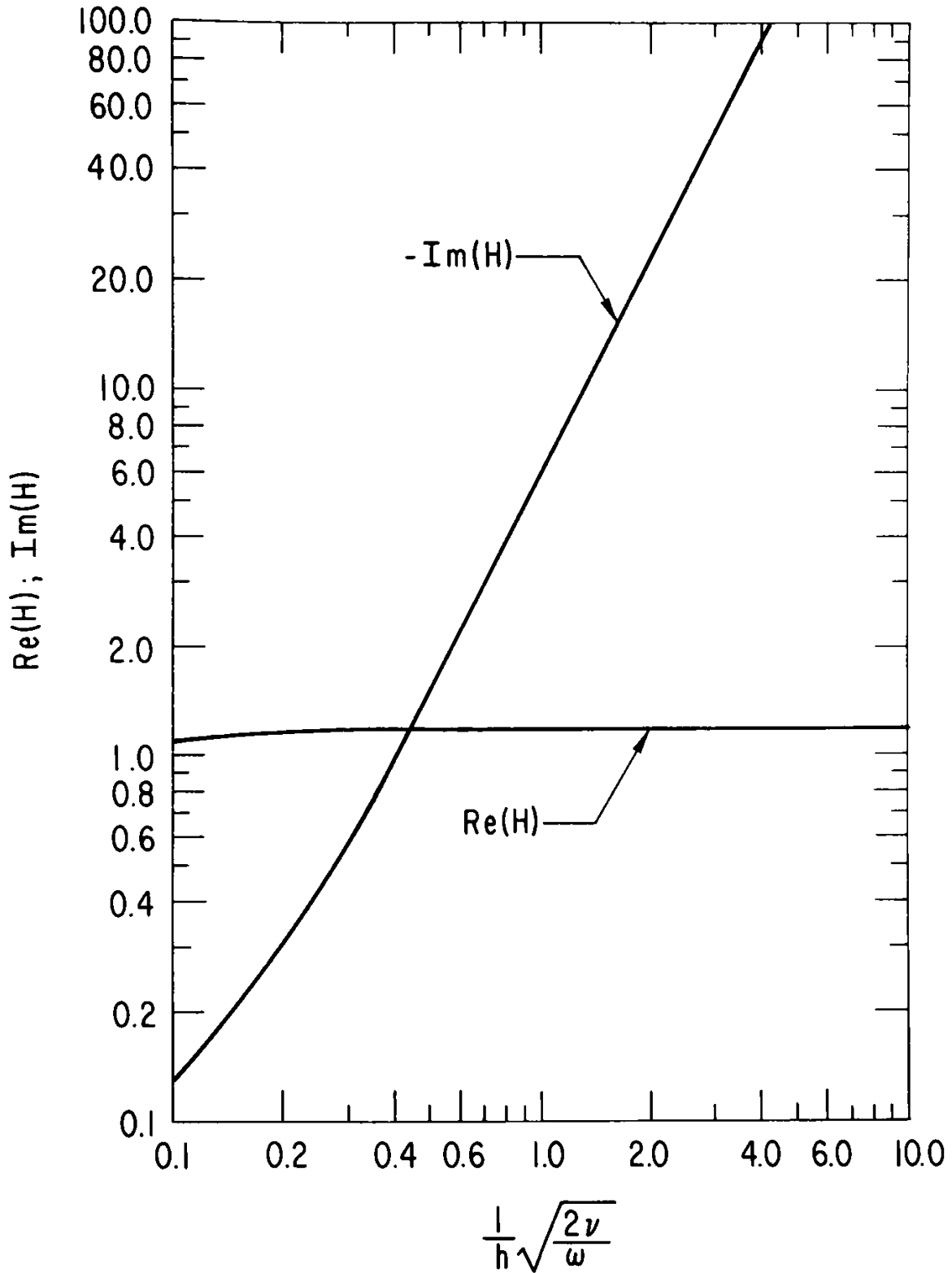
Fig. 7. Added mass and damping multipliers, Re(H) and Im(H) [Ref. 8].
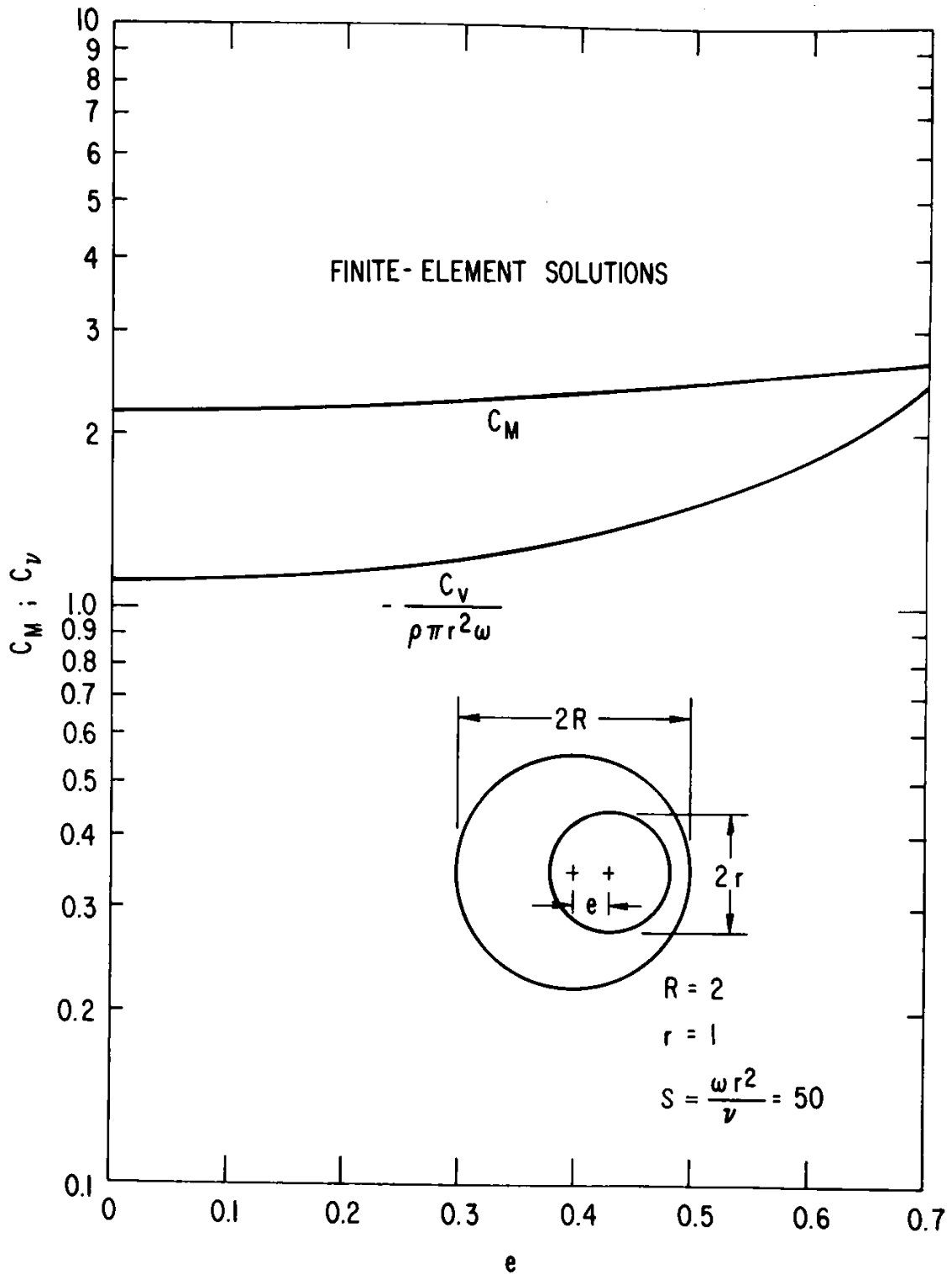
Fig. 8.   Added mass and damping coefficient as a function of eccentricity
          [Ref. 9].

$a = \dfrac{\omega r}{c}$ (c = velocity of sound),

$\Delta = [J_2(a) - J_0(a)]^2 + [Y_2(a) - Y_0(a)]^2$,

$\Delta_1 = J_1(a)[J_2(a) - J_0(a)] + Y_1(a)[Y_2(a) - Y_0(a)]$, and

$\Delta_2 = Y_1(a)[J_2(a) - J_0(a)] - J_1(a)[Y_2(a) - Y_0(a)]$.

The values of C_M and C_v are given in Fig. 9.

For a uniform cylinder with mass per-unit length m, the modal damping ratio attributed to fluid compressibility is

$$\zeta_n = \left(\dfrac{M_d}{m}\,\Delta_2\right) / \left[a\Delta + 2\left(\dfrac{M_d}{m}\right)\Delta_1\right] .\tag{13}$$

5. Two Coaxial Circular Cylinders Separated by Viscous Fluid

Fluid forces acting on two coaxial tubes separated by an incompressible fluid are obtained based on the linearized two-dimensional Navier-Stokes equation [Ref. 5]. The fluid forces acting on the two cylinders are (Fig. 10)

$$f_i = \sum_{j=1}^{2} \left(\alpha_{ij}\,\dfrac{\partial^2 u_j}{\partial t^2} + \alpha'_{ij}\,\dfrac{\partial u_j}{\partial t}\right) ,\tag{14}$$

$$\alpha_{ij} = \rho\pi R_i R_j \text{Re}(a_{ij}),$$

$$\alpha'_{ij} = \rho\pi R_i R_j \omega \text{Im}(-a_{ij}) ,$$

$$a_{11} = -(1 + 2a) ;\tag{15}$$
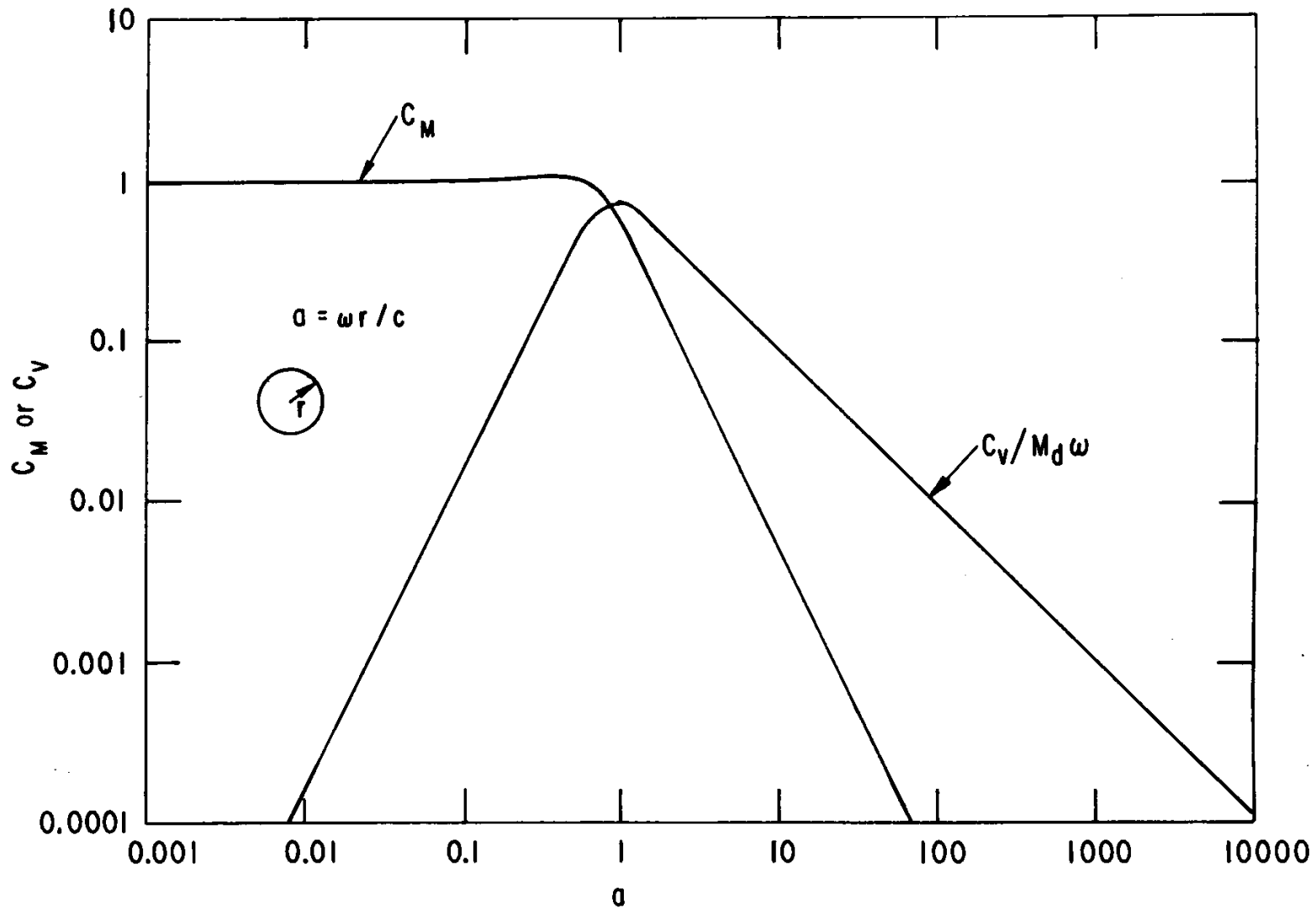
Fig. 9. C_M and C_v as functions of $\omega r/c$ for a cylinder vibrating in an infinite compressible fluid.
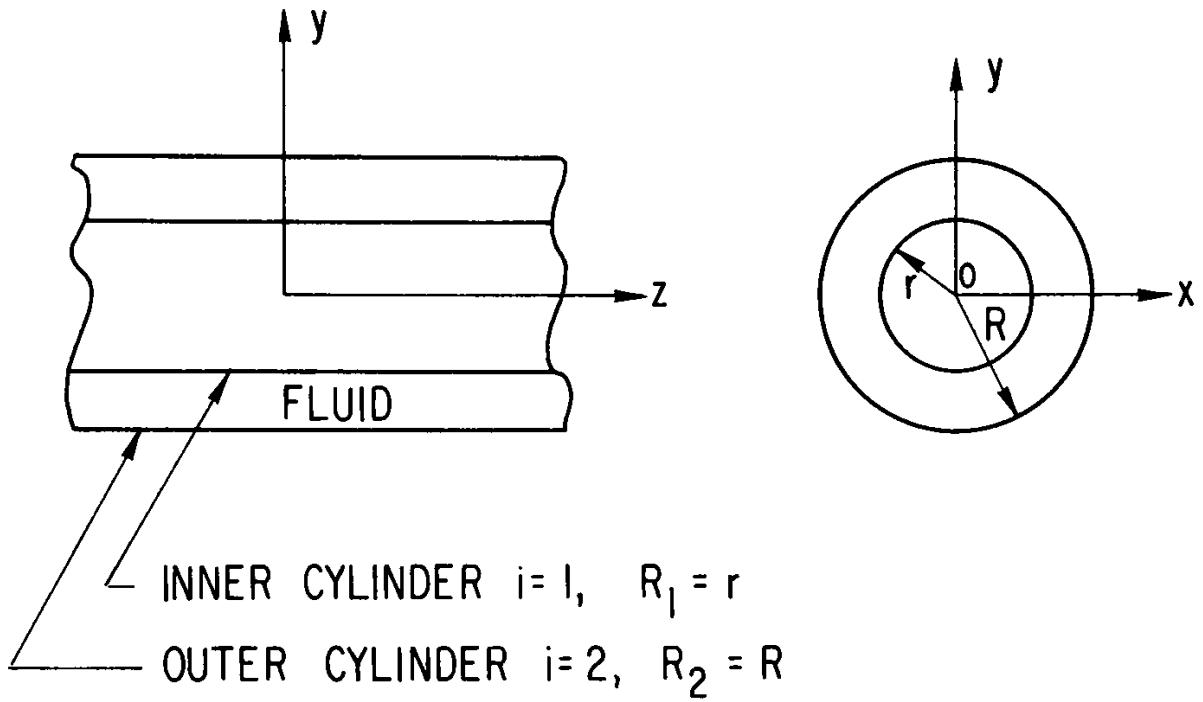
Fig. 10. Schematic of two concentric cylinders containing viscous fluid.

$$a_{12} = a_{21} = 2\gamma a = -\gamma(1 + a_{11}) \; ,$$

$$a_{22} = 1 - 2\gamma^2 a = 1 + \gamma^2(1 + a_{11}) \; ,$$

$$b_i = (-i\omega/\nu)^{1/2} R_i \; , \tag{15}$$

(Contd.)

$$\gamma = r/R \; , \text{ and}$$

$$
a = - \begin{vmatrix} 1 & 1 & F_1(b_1) & G_1(b_1) \\ 0 & 1 & \gamma F_1(b_2) & \gamma G_1(b_2) \\ 2 & 2 & b_1 F_0(b_1) & b_1 G_0(b_1) \\ 0 & 2 & b_1 F_0(b_2) & b_1 G_0(b_2) \end{vmatrix} \div \begin{vmatrix} 1 & 1 & F_1(b_1) & G_1(b_1) \\ \gamma^2 & 1 & \gamma F_1(b_2) & \gamma G_1(b_2) \\ 0 & 2 & b_1 F_0(b_1) & b_1 G_0(b_1) \\ 0 & 2 & b_1 F_0(b_2) & b_1 G_0(b_2) \end{vmatrix} \; ,
$$

where F_n and G_n are the nth-order Bessel functions. They can be either the first- and second-kind Bessel functions, J_n and Y_n, or the Hankel functions, $H_n^{(1)}$ and $H_n^{(1)}$. The selection of the functions mainly depends on computational considerations.

The coefficients α_{ij} and α'_{ij} depend on the $S(= \omega r^2/\nu)$ and γ in a very complicated way. Approximate solutions can be obtained in special cases:

(a) <u>Viscous fluid and very large radius ratio (e.g., $\gamma > 10$, $S > 1$)</u>

For $\gamma \to 0$ and $|b_2| \gg 1$,

$$a_{11} = 1 - 4H_1^{(2)}(b_1)/b_1 H_0^{(2)}(b_1) \; . \tag{16}$$

Furthermore, if $|b_1| \gg 1$,

$$a_{11} = 1 - \frac{4i}{b_1} \; . \tag{17}$$

(b) <u>Viscous fluid and large value of S (e.g., $S > 10^4$)</u>

$$a_{11} = -1 + \{[16b_1^2 - (73 - 578\gamma + 9\gamma^2)/8]\sin(Gb_1)$$

$$- 2b_1(1 - \gamma)(16 + \sqrt{\gamma})\cos(Gb_1)\}$$

$$\div \{(1 - \gamma^2)[8b_1^2 - (9 + 30\gamma + 9\gamma^2)/16]\sin(Gb_1)$$

$$+ b_1(1 + \gamma)(1 + 14\gamma + \gamma^2)\cos(Gb_1) - 32b_1\gamma\sqrt{\gamma}\} , \qquad (18)$$

$$G = (1 - \gamma)/\gamma .$$

(c) <u>$S \gg 1$ and $G^2S \ll 1$</u>

$$a_{11} = -12i/G^3S . \qquad (19)$$

(d) <u>$S \gg 1$ and moderate gap (e.g., $G > 0.01$ and $S > 10^4$)</u>

$$a_{11} = \frac{b_1(1 + \gamma^2)\sin(Gb_1) - 2(2 - \gamma + \gamma^2)\cos(Gb_1) + 4\gamma\sqrt{\gamma}}{b_1(1 - \gamma^2)\sin(Gb_1) + 2\gamma(1 + \gamma)\cos(Gb_1) - 4\gamma\sqrt{\gamma}} . \qquad (20)$$

(e) <u>$S \gg 1$ and $G^2S \gg 1$ (e.g., $S > 10^4$, and $G^2S > 10^4$)</u>

$$a_{11} = [b_1(1 + \gamma^2)$$

$$- i2(2 - \gamma + \gamma^2)]/[b_1(1 - \gamma^2) + i2\gamma(1 + \gamma)]. \qquad (21)$$

(f) <u>$S \gg 1$, $G^2S \gg 1$ and $G \ll 1$ (e.g., $S > 10^7$, $G^2S > 10^4$ and $G < 0.05$)</u>

$$a_{11} = \frac{1 + \gamma^2}{1 - \gamma^2} + \frac{\sqrt{2}}{G^2S^{1/2}}\left[1 - i\left(1 - \frac{4\sqrt{2}}{S^{1/2}}\right)\right] . \qquad (22)$$

(g) <u>$\nu \to 0, S \to \infty$</u>

$$a_{11} = \frac{1 + \gamma^2}{1 - \gamma^2} . \qquad (23)$$

6. **Cylinder Arrays in Incompressible Viscous Fluid**

The viscous damping coefficient matrices α'_{ij}, σ'_{ij}, τ'_{ij}, and β'_{ij} for general cylinder arrays can be calculated based on the linearized two-dimensional Navier-Stokes equation.

There are several experimental studies on the damping of multiple cylinders. Shimogo et al. [11] present the results of two cylinders vibrating in a viscous fluid. The effects of fluid viscosity on tube motions are studied. A series of experiments to study the diagonal terms, α'_{ij} and β'_{ij} is reported by Chen et al. [12].

For cylinder arrays vibrating in a quiescent fluid, α'_{ij} and β'_{ij} are symmetric, and $\tau'_{ij} = \sigma'_{ji}$. Physically, this means that the damping of cylinder i due to the motion of cylinder j is equal to the damping of cylinder j due to the motion of cylinder i.

It should be pointed out that in a viscous fluid, the motion of a cylinder is coupled to other cylinders in an array through added mass coupling and viscous coupling as given in Eq. 2, where [M] represents the mass effect and [C] represents the viscous damping. In general, [C] is not proportional to [M].

For a group of N cylinders, there are N^2 elements of damping coefficients. It is impractical to compile all available data in this design guide. In fact, there are practically no complete data for any cylinder arrays consisting of more than three cylinders. In most cases, it is not practical to calculate all these coefficients. However, if the detailed damping coefficients are needed, the finite element method can be applied.

7. **An Infinite Circular Cylinder in a Concentric Annular Two-Phase Flow**

A circular cylinder vibrating in a confined two-phase flow was studied experimentally by several investigators [13-16]. The inertia and damping forces can be written

$$f = C_M M_d \frac{d^2u}{dt^2} + (C_v + C_t) \frac{du}{dt} \ . \tag{24}$$

Note that Eq. 24 is the same as Eq. 5 with the additional term $C_t(du/dt)$, called the two-phase-flow damping. However, the added mass coefficient C_M and viscous damping coefficient C_v are not the same as those for a single-phase flow. Based on the limited experimental data, and on analytical results, C_M can be calculated based on Eq. 6 with the exception that the effective density should be used. The ratio of effective density ρ_e to that of the single-phase flow ρ is given in Fig. 11, which includes experimental data and analytical results. The theoretical values ρ_e of the effective density are given by

(1) $\rho_e = (1 - \alpha_e)\rho + \alpha_e\rho'$,   (25a)

(2) $\rho_e = \rho(1 - \alpha_e)/(2\alpha_e + 1)$,   (25b)

(3) $\rho_e = \rho(1 - \alpha_e)(1 + 2\alpha_e)/(1 + 4\alpha_e - 2\alpha_e^2)$,   (25c)

where α_e is the void fraction, and ρ and ρ' are the densities of the two fluids. Equation 25a is applicable for small α_e; at large α_e, it predicts much larger ρ_e than the experimental data. Equations 25b and 25c correlate better with the experimental data at high values of α_e and are applicable in that range.

The coefficient C_v in Eq. 24 for two-phase flow is calculated following the single-phase flow described in Section III.1. However, the effective density ρ_e given in Eq. 25a and the mixture kinetic viscosity based on McAdams' definition [17] should be used.[*]

There is no analytical expression for C_t. The most complete experimental data are those by Carlucci and Brown [14]; these data are given in Fig. 12. With Fig. 12, the two-phase damping coefficient C_t can be calculated based on C_v.

The added mass and damping of circular cylinders vibrating in a two-phase flow are still not well understood. More theoretical and experimental

---

[*]The mixture viscosity according to McAdams is given by the following equation:

$$\frac{1}{\mu_{mixture}} = \frac{\alpha_e}{\mu_{vapor}} + \frac{(1 - \alpha_e)}{\mu_{liquid}} .$$
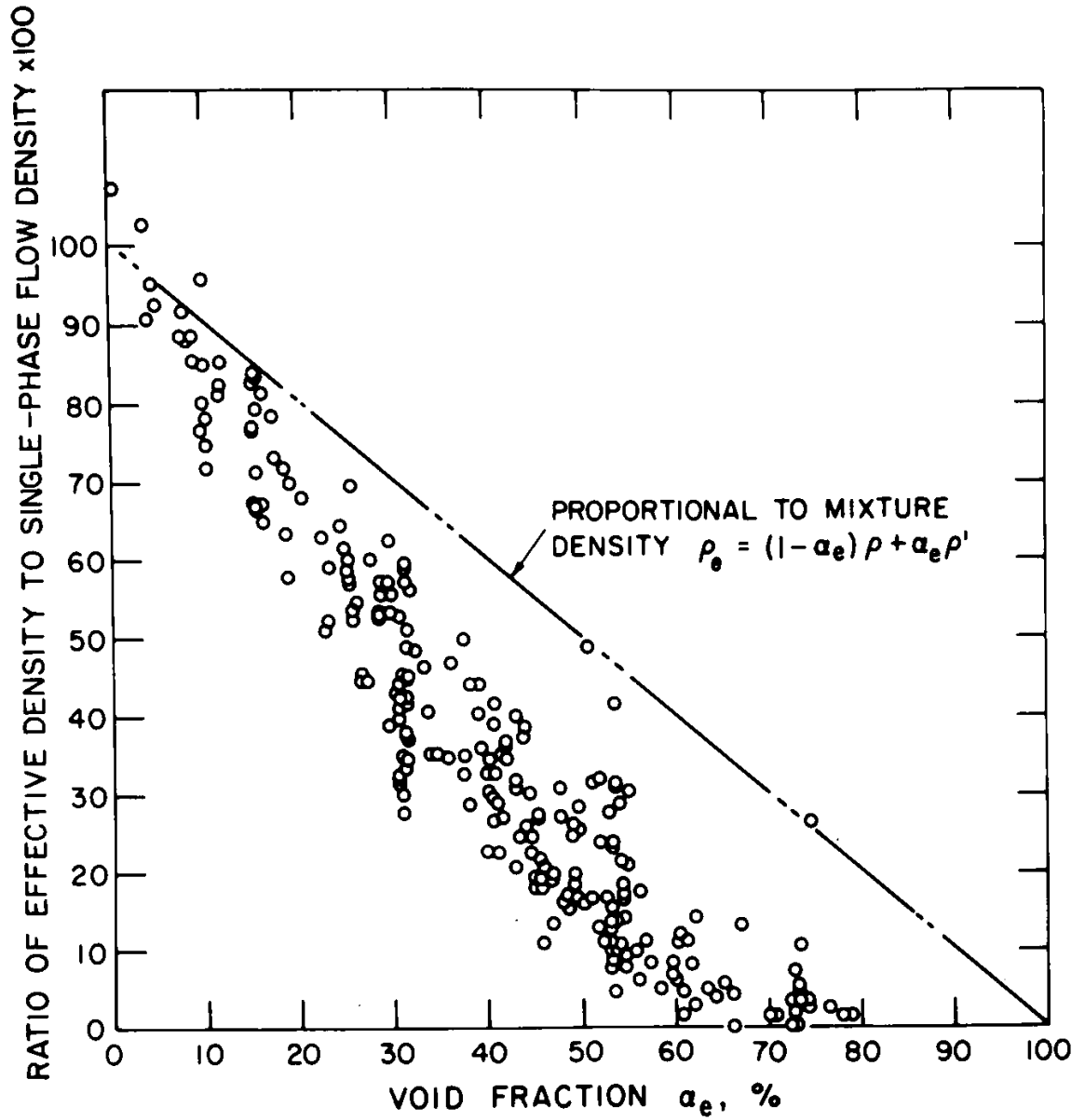
Fig. 11. Effective density for two-phase flow as a function of void fraction.

33

Fig. 12. Viscous damping coefficient for two-phase flow.
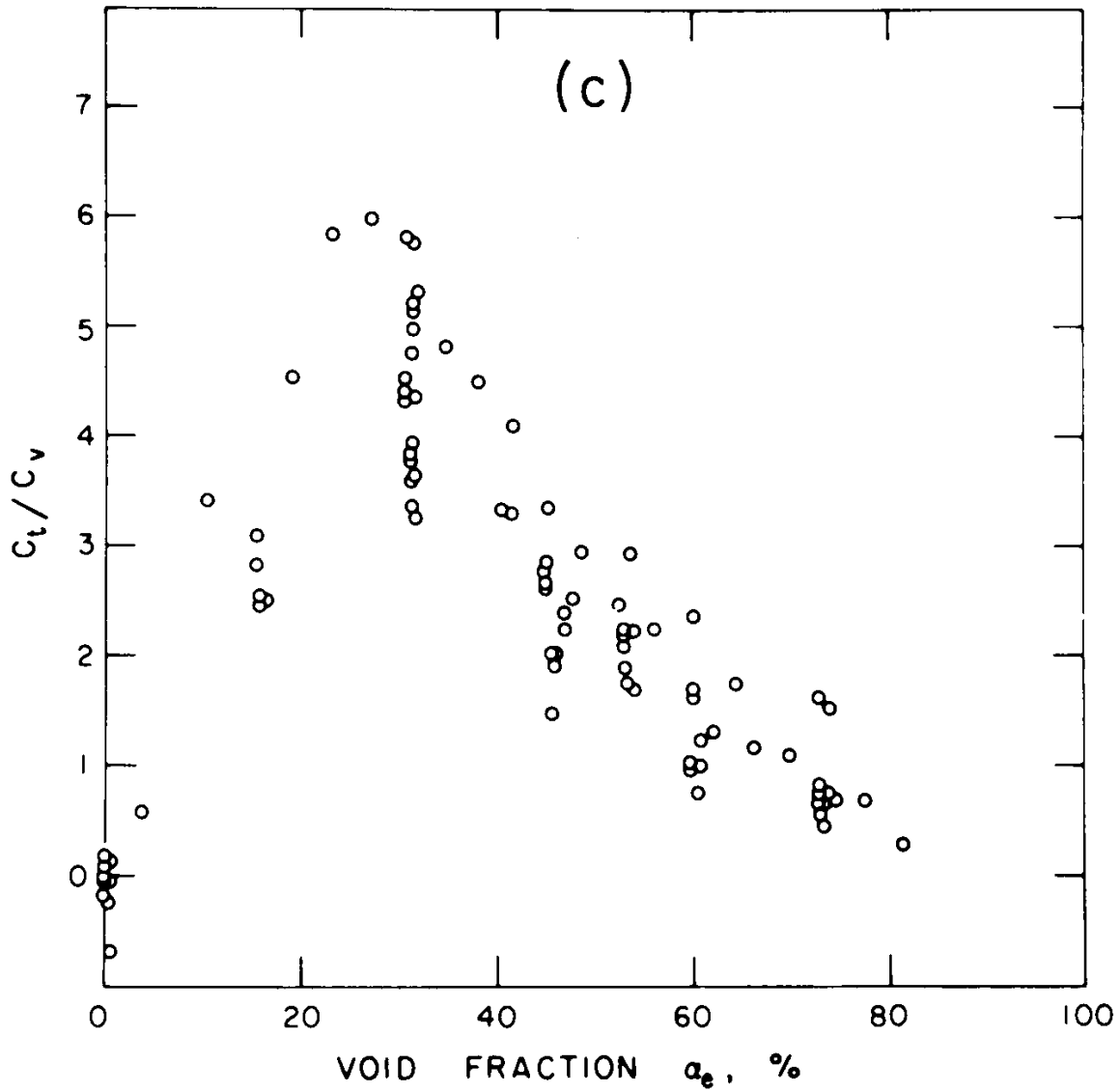
studies are needed; in particular, there are practically no experimental data for cylinder arrays.

8. Circular Cylindrical Shells

For small-amplitude oscillatory motion, the fluid damping force may be calculated based on the linearized viscous flow theory. The results are very complicated, in general, and the details of the analytical and experimental results cannot be included in this design guide. The following text includes several cases that may be of some use in determining the role of fluid damping.

a. An Infinitely Long Cylindrical Shell Surrounded by Compressible Fluid

The response of this type of shell in fluid to an excitation can be analyzed using the cylindrical shell theory and inviscid compressible flow theory [18]. Depending on the frequency range, the solution may be of a traveling or a stationary wave type. Let c = velocity of sound in fluid, ℓ = axial half wavelength, and ω = oscillation frequency. Then for $\omega > c\pi/\ell$, it is a traveling wave solution; the energy carried away will contribute to damping of the shell. For $\omega < c\pi/\ell$, it is a stationary wave solution; no energy will be carried away by the acoustic medium.

b. Two Infinitely Long Coaxial Cylindrical Shells Coupled by Viscous Fluid

An analysis is presented for coupled vibration of two concentric shells separated by a viscous fluid [19]. The coupling effects are accounted for by using a fluid stress coefficient matrix of concentric shells. With this type of analysis, the natural frequencies and modal damping ratio of coupled, concentric shells in viscous fluid can readily be obtained.

The lowest natural frequency of the coupled shell system with fluid is significantly lower than those of the individual shells. The frequencies of the first coupled modes (out-of-phase modes—the two shells moving out of phase with respect to each other) are lower than either of the uncoupled natural frequencies. The effect of the fluid viscosity on the system natural frequencies is negligibly small in most practical systems.

However, the modal damping ratio is noticeably increased for some cases when the fluid viscosity is included, especially for the lower-frequency cases. For a coupled shell, the viscous effects are most pronounced for the out-of-phase modes, but these effects are considered to be negligible for the in-phase mode. In general, the effect of fluid viscosity on damping can be estimated based on the corresponding structure vibrating in an infinite fluid for the radius ratio of the two shells larger than 1.15. However, if it is less than 1.15, the viscous damping should be calculated based on the coupled mode.

c.   Two Finite-Length Coaxial Cylindrical Shells Coupled by Viscous Fluid

The natural frequencies and modal damping ratio of two coaxial cylindrical shells of finite length are determined in tests by several investigators [20,21]. The modal damping ratio depends on different modes. In general, the results are consistent with the analytical results obtained for the infinite shells [19]; i.e., there is a significant increase in damping ratios of the shell system as the gap decreases for the out-of-phase modes, but only a moderate increase for the in-phase modes.

9.   Cylinder Arrays in Compressible Fluid

The radiation damping for cylinder arrays depends on arrangement and wave number λr (r = cylinder radius, $\lambda = \omega/c$, ω = oscillation circular frequency, and c = speed of sound). A general method of analysis to determine fluid damping for a group of cylinders is available [22]. The perturbed fluid motion is described by a two-dimensional acoustic wave equation with Newmann conditions on the cylinders and the radiation condition at infinity. The solution is in terms of a series of cylindrical wave functions associated with the polar coordinates of each cylinder. To satisfy the boundary conditions on a particular cylinder, all cylindrical wave functions are transformed to the local coordinates of that cylinder. The resulting equations are a system of linear algebraic equations for the undetermined constants that are then solved numerically by a digital computer.

In general, for small values of λr (e.g., 0.01), incompressible flow theory is a valid approximation for determining added mass and the radiation

damping is approximately zero. For $\lambda r > 0(1)$, the values of added mass are relatively small and the effect of radiation damping will be dominant.

Other techniques can also be used to study the damping, e.g., T-matrix approach [23].

10. Effects of Other Parameters

The results presented in Sections III.1 through III.9 are applicable to small-amplitude oscillations; i.e., the structure displacement must be much smaller than a characteristic length, such as cylinder diameter, clearance between two cylinders, or shell radius. When the displacement becomes large, nonlinear effects will become important.

a. Nonlinear Effect of a Cylinder Oscillating in an Infinite Fluid

The added mass and damping of a cylinder are studied in detail by Skop et al. [24]. The added mass coefficient C_M (see Eq. 5) is essentially equal to 1, as predicted by linear theory. For vibrational amplitudes less than 0.4 cylinder diameter, the fluid damping force is essentially viscous and can be calculated based on the equation given in Section III.1. However, for $\beta_a > 0.4$ (β_a = oscillation amplitude/cylinder diameter), the fluid damping contains both linear and velocity-squared components. The viscous damping coefficient C_v to account for the large amplitude oscillations is given as follows:

$$C_v = \pi \rho \sqrt{\omega \nu} \left[4.5 + 0.91 \left(\frac{\omega r^2}{\nu}\right)^{0.5} (\beta_a - 0.4) \right] H(\beta_a - 0.4) , \qquad (26)$$

where ρ = fluid density, ω = oscillation frequency, ν = kinetic viscosity, r = cylinder radius, and H is the Heaviside unit step function. Equation 26 is determined from experimental data obtained for $230 < \omega r^2/\nu < 5220$.

For large-amplitude vibrations, the results presented in Section III are not strictly applicable, and there are very few data available for large-amplitude oscillations. Fortunately, in most practical applications, one is more interested in the small-amplitude oscillations, since the large-amplitude vibration is not acceptable in general. In addition, linear theory is also valid to determine the stability-instability boundary.

b. Scale Model

The current state-of-the-art knowledge of vibration of cylinders in flow is not well enough developed to rely solely upon analytical predictions; therefore, scale-model testing is employed frequently for design verification. Fluid damping is one of the parameters that is difficult to scale.

Small-scale models frequently are used in practice for design evaluation. The kinetic Reynolds number $S(= \omega r^2/\nu)$ has to be simulated to obtain proper fluid damping. However, in most cases, other parameters, such as Strouhal number, may be more important. It is very difficult to simulate all the parameters simultaneously. In this situation, the kinetic Reynolds number has to be distorted. Considerations must be made to account for the scaling effect on fluid damping. In general, a small-scale model will give a larger value of fluid damping that is not conservative.

IV. PARALLEL FLOW

In a flowing fluid, in addition to the damping associated with fluid viscosity and fluid compressibility, a damping attributed to flow velocity, called flow-velocity-dependent damping, is important. In this section and the next one on crossflow, the flow-velocity-dependent damping will be discussed. Therefore, in a flowing fluid, the total damping is the sum of damping in stationary fluid plus flow-velocity-dependent damping.

1. Tubes Conveying Fluid

Consider a uniform straight tube with mass per unit length m, and flexural rigidity EI, conveying fluid of mass per unit length M_f flowing axially with velocity V (see Fig. 13). The linear equation of motion is [25,26]

$$EI \frac{\partial^4 u}{\partial z^4} + M_f V^2 \frac{\partial^2 u}{\partial z^2} + 2M_f V \frac{\partial^2 u}{\partial z \partial t} + C_s \frac{\partial u}{\partial t} + (m + M_f) \frac{\partial^2 u}{\partial t^2} = 0 \ . \tag{27}$$

Let

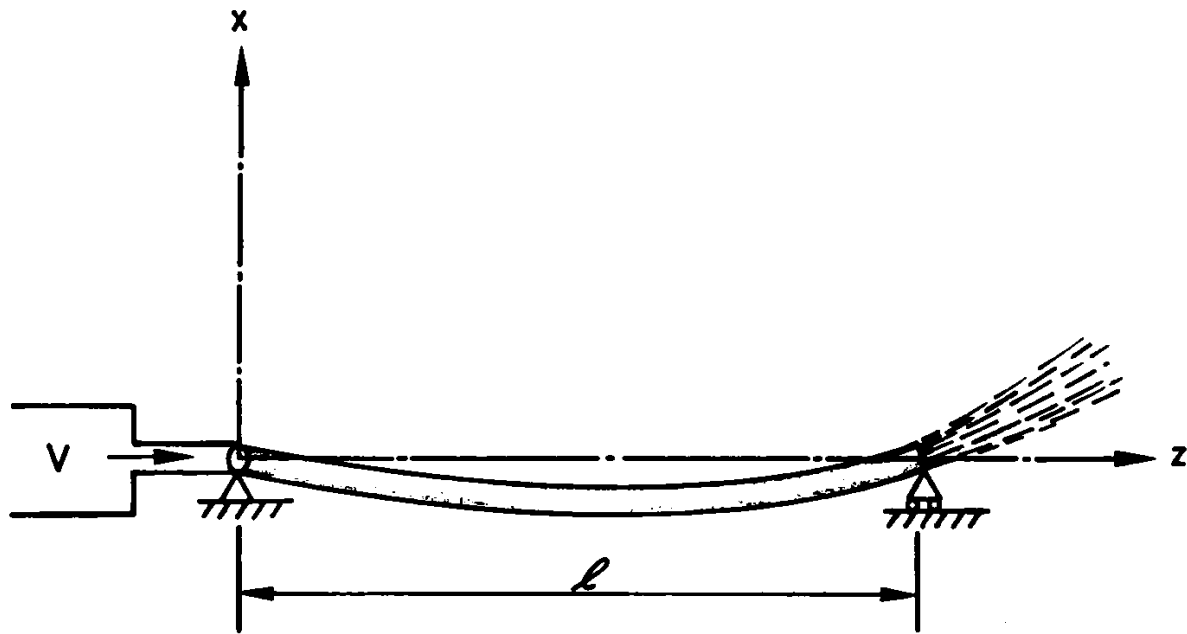$$u(z,t) = \sum_{i=1}^{\infty} q_i(t) \phi_i(z) \ , \tag{28}$$

Fig. 13.   Schematic of a tube conveying fluid.

where $\phi_i(z)$ is the orthonormal modal function without the effect of the Coriolis force. Equation 27 can be reduced to a system of coupled equations using Eq. 28:

$$\ddot{q}_n + 2\delta\dot{q}_n + 2\lambda V \sum_{j=1}^{\infty} c_{nj}\dot{q}_j + \omega_n^2 q_n = 0, \tag{29}$$

where ω_n is the dimensionless natural frequency of nth mode without the effect of the Coriolis force, and

$$c_{nj} = \frac{1}{\ell} \int_0^{\ell} \frac{d\phi_j(z)}{dz} \phi_n(z)dz \ ,$$

$$\lambda = \frac{M_f}{(m + M_f)} \ , \tag{30}$$

and

$$\delta = \frac{C_s}{2(m + M_f)} \ .$$

Note that Eqs. 29 are coupled; the coupling arises from the Coriolis force. Because of the Coriolis force, the system does not possess classical normal modes, in which the various parts of the system pass through the equilibrium position at the same instant of time. In addition, the Coriolis force may act as a damping mechanism.

From Eq. 30, it follows that:

$$c_{nj} + c_{jn} = \phi_n(\ell)\phi_j(\ell) - \phi_j(0)\phi_n(0) \ . \tag{31}$$

If the tube is not movable at the ends,

$$c_{nj} = -c_{jn} \ . \tag{32}$$

The work done by the Coriolis force is

$$\Delta W = -2\lambda V \sum_n \sum_j c_{nj}\dot{q}_n\dot{q}_j dt \ . \tag{33}$$

If the tube is not allowed to move at the ends, Eq. 32 is satisfied and $\Delta W = 0$; the Coriolis force does not dissipate or supply any energy to the

system and is not a damping mechanism. However, if the tube is allowed to move at the end, the Coriolis force is a damping mechanism.

Alternatively, this can also be demonstrated as follows: the Coriolis force is given by

$$f(z,t) = -2M_f V \frac{\partial^2 u}{\partial z \partial t} \ . \tag{34}$$

The work done by the Coriolis force is

$$\Delta W = \int_0^u \int_0^\ell f(z,t) du \ dz$$

$$= -2M_f V \int_0^t \int_0^\ell \frac{\partial^2 u}{\partial z \partial t} \frac{\partial u}{\partial t} dt \ dz$$

$$= -M_f V \int_0^t \left(\frac{\partial u}{\partial t}\right)^2 dt \Big|_0^\ell \ . \tag{35}$$

As long as there is no movement at the ends, $\Delta W = 0$ and the Coriolis force is not a damping mechanism.

For tubes allowed to move at the ends, the modal damping ratio attributed to the Coriolis force is approximately

$$\zeta_n = \frac{M_f V}{(m + M_f) \omega_n \ell} \int_0^\ell \frac{d\phi_n(z)}{dz} \phi_n(z) dz \ . \tag{36}$$

Equivalently, the damping coefficient C_v attributed to the Coriolis force is

$$C_v = \frac{2M_f V}{\ell} \int_0^\ell \frac{d\phi_n(z)}{dz} \phi_n(z) dz \ . \tag{37}$$

Damping is proportional to flow velocity and fluid mass per unit length inside the tube.

In summary, the effects of the damping associated with the Coriolis force are as follows:

• For tubes that are not movable at the ends, the Coriolis force is not a damping force; its effect is to induce phase distortion such that the tube-fluid system does not possess classical normal modes.

• For tubes that are movable at the ends, the Coriolis force may become a damping force. For a given mode, the damping value increases with the flow velocity. For example, in a cantilevered tube conveying fluid, the damping attributed to the Coriolis force can become very large and the tube is overdamped in the first mode [27].

For curved tubes, either vibrating in the in-plane or out-of-plane directions, fluid Coriolis forces also play the same role as that in a straight tube. Consider a uniformly curved tube conveying fluid as shown in Fig. 14. The tube has radius of curvature R, mass per unit length m, flexural rigidity EI, torsional rigidity GJ, and subtended angle α, conveying fluid of mass per unit length M_f. The equations of motion for the four displacement components are [28,29]

In-plane motion (inextensional theory):

$$\frac{EI}{R^3} \left(\frac{\partial^6 w}{\partial \theta^6} + 2 \frac{\partial^4 w}{\partial \theta^4} + \frac{\partial^2 w}{\partial \theta^2} \right) + \frac{M_f V^2}{R} \left(\frac{\partial^4 w}{\partial \theta^4} + 2 \frac{\partial^2 w}{\partial \theta^2} + w \right)$$

$$+ 2 M_f V \left(\frac{\partial^4 w}{\partial \theta^3 \partial t} + \frac{\partial^2 w}{\partial \theta \partial t} \right) + R(m + M_f) \left(\frac{\partial^4 w}{\partial \theta^2 \partial t^2} - \frac{\partial^2 w}{\partial t^2} \right) = 0 \qquad (38)$$

and

$$u = \frac{\partial w}{\partial \theta} .$$

Out-of-plane motion:

$$\frac{EI}{R^3} \left(\frac{\partial^4 v}{\partial \theta^4} - R \frac{\partial^2 \phi}{\partial \theta^2} \right) - \frac{GJ}{R^3} \left(\frac{\partial^2 v}{\partial \theta^2} + R \frac{\partial^2 \phi}{\partial \theta^2} \right) + \frac{MV^2}{R} \frac{\partial^2 v}{\partial \theta^2}$$

$$+ 2MV \frac{\partial^2 v}{\partial \theta \partial t} + R(m + M) \frac{\partial^2 v}{\partial t^2} = 0$$

and $\qquad\qquad\qquad\qquad\qquad\qquad\qquad\qquad\qquad\qquad\qquad\qquad (39)$

$$\frac{EI}{R^2} \left(R \phi - \frac{\partial^2 v}{\partial \theta^2} \right) - \frac{GJ}{R^2} \left(R \frac{\partial^2 \phi}{\partial \theta^2} + \frac{\partial^2 v}{\partial \theta^2} \right) = 0 .$$
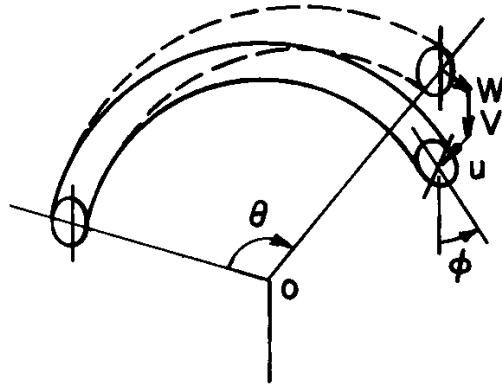
(b)STRESSED STATE
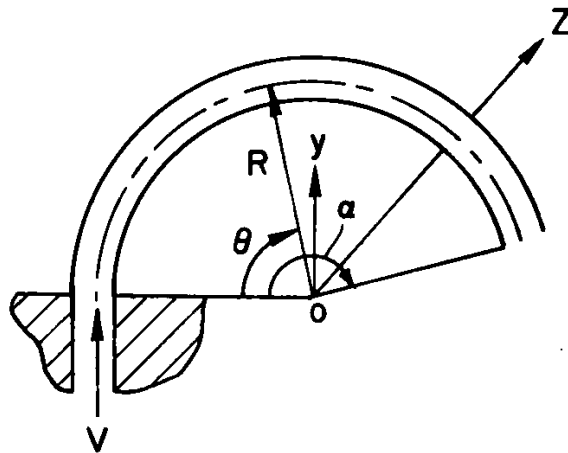
(a)UNSTRESSED STATE

Fig. 14. Definition of coordinates and displacements of a uniformly curved
          tube conveying fluid.

The force component $2M_f V \left(\dfrac{\partial^4 w}{\partial\theta^3 \partial t} + \dfrac{\partial^2 w}{\partial\theta \partial t}\right)$ in Eq. 38 and $2M_f V \dfrac{\partial^2 v}{\partial\theta \partial t}$ in Eq. 39 are attributed to the Coriolis force. The effect of these fluid forces is similar to that of a straight tube.

Tubes conveying pulsating flow [30-32] and two-phase flow [33] also have been studied. The results of fluid damping are rather complicated and cannot be included in this design guide.

2. A Single Cylinder Submerged in Parallel Flow

For a single cylinder submerged in axial flow, the flow-velocity dependent damping force is [34]

$$f = 2M_f V \frac{\partial^2 u}{\partial z \partial t} + \frac{1}{2} C_N \frac{M_f V}{D} \frac{\partial u}{\partial t} , \tag{40}$$

where C_N is the drag coefficient. The first term is the Coriolis force, and the second term is the drag-induced damping. The modal damping ratio attributed to the flow-velocity-dependent force for a uniform rod with mass per unit length m is given by

$$\zeta_n = \frac{M_f V}{(m + m_f) \omega_n \ell} \int_o^\ell \frac{d\phi_n(z)}{dz} \phi_n(z) dz + \frac{M_f V C_N}{4D\omega_n (m + M_f)} . \tag{41}$$

The damping coefficient C_v attributed to the Coriolis force and drag force is

$$C_v = \frac{2M_f V}{\ell} \int_o^\ell \frac{d\phi_n(z)}{dz} \phi_n(z) + \frac{1}{2} C_N \frac{M_f V}{D} . \tag{42}$$

The damping attributed to the Coriolis force is the same as that of tube conveying fluid (see Eq. 37).

Two typical examples of modal damping ratios are given in Figs. 15 and 16 for a fixed-fixed cylinder and a cantilevered cylinder [34]. Figures 15 and 16 show the total damping. For the fixed-fixed cylinder, the contribution from the Coriolis force is zero; therefore, the increase of damping with flow velocity is attributed to the drag force (second term in Eq. 42). For the cantilevered cylinder, the Coriolis force contributes significantly to the damping. Consequently, the total damping is much
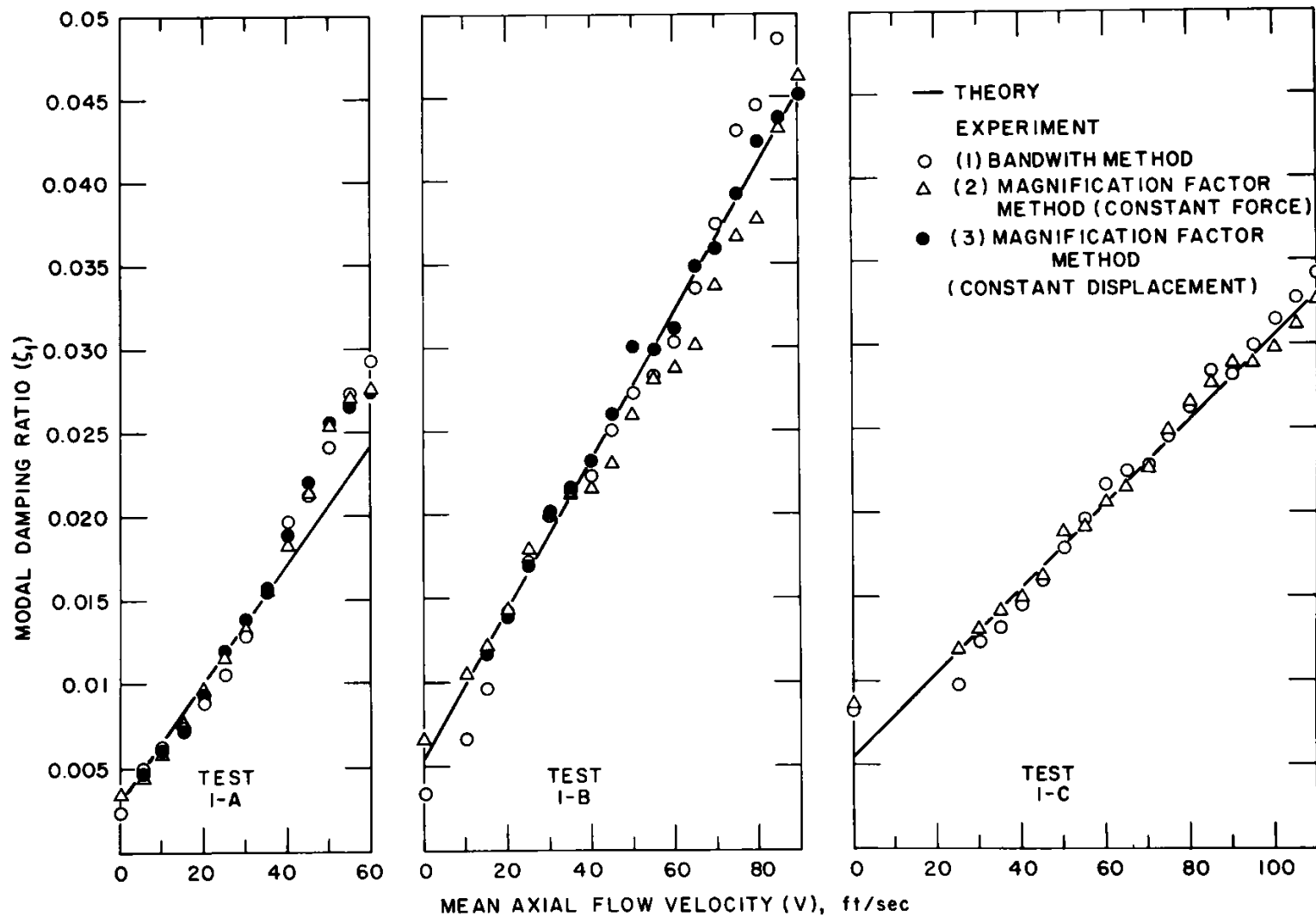
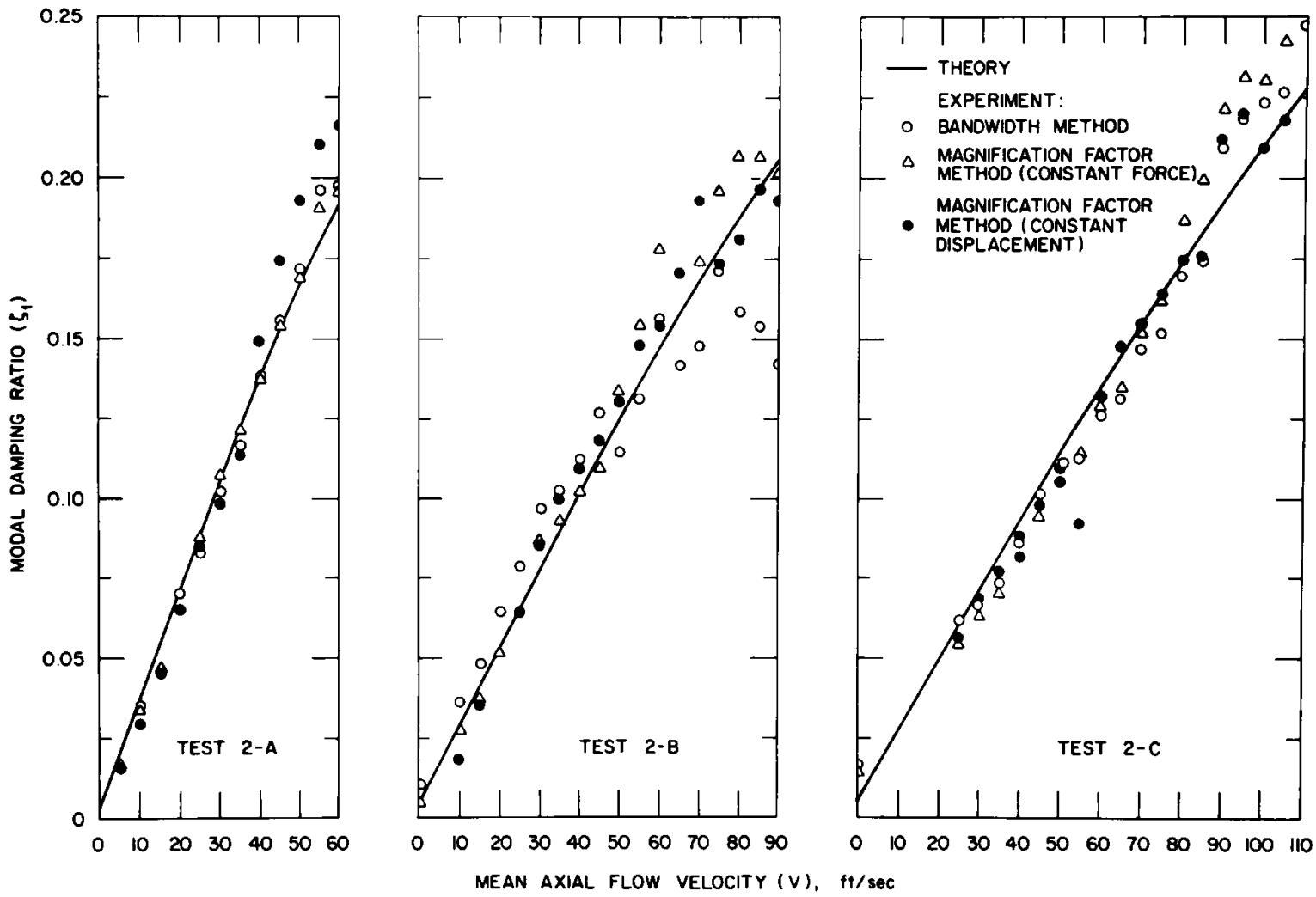Fig. 15. Modal damping ratio of a fixed-fixed cylinder.

Fig. 16.   Modal damping ratio of a cantilevered cylinder.

larger than that of the fixed-fixed cylinder. In the flow velocity range tested the theoretical model agrees well with experimental data.

The values of C_N obtained for several cases are given in Table 1. These tests were conducted for a cylinder vibrating in an annual region with the radius ratio of 1.24 to 4.0.

The effect of trailing-end geometry on the damping of a cantilevered cylinder is important. Eleven different trailing-end geometries were studied by Wambsganss and Jendrzejczyk [35]. The total modal damping ratio was given by

$$\zeta = b + cV . \tag{43}$$

The values of b and c are given in Table 2. The second term is the resultant effect of the Coriolis force, drag force, and end effect. Equation 43 can be written

$$\zeta = b + c_c V + c_d V + c_e V . \tag{44}$$

The damping attributed to the Coriolis force $c_c V$ and drag force $c_d V$ do not change with end geometry; therefore, the variation in cV is attributed to the end effect. The coefficients c_c and c_d can be calculated from Eqs. 41:

$$c_c = \frac{M_f}{(m + m_f)\omega_n \ell} \int_o^\ell \frac{d\phi_n(z)}{dz} \phi_n(z) dz ,$$

and
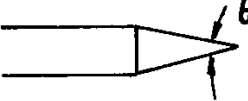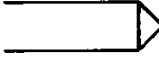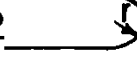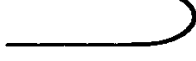
$$c_d = \frac{M_f C_N}{4 D \omega_n (M_f + m)} . \tag{45}$$

Because most of these parameters are not available, c_e can be approximately calculated as follows. The damping for the tapered end ($\theta = 30°$) increases most slowly with the flow velocity. It is assumed that c_e is zero for this case. Then c_e for other cases can be calculated; the result is given in Table 2.

Table 1. Drag coefficient C_N for a cylinder in an annular region

Investigators	Support Condition of Cylinder	Radius Ratio R/r	C_N	Remarks
Chen and Wambsganss [34] (1972)	Clamped-Clamped	4	0.101	Brass Tube
		3	0.103	Brass Tube
		2	0.044	Brass Tube
	Clamped-Free	4	0.10	Brass Tube
		3	0.056	Brass Tube
		2	0	Brass Tube
	Clamped-Clamped	2	0.025	Steel Tube
Carlucci [13] (1980)	Clamped-Clamped	1.57	0.071	Brass Tube
		1.24	0.085	Brass Tube

Table 2. Empirical relationships for damping as a function of mean
axial flow velocity [35]

TRAILING END GEOMETRY	$b \times 10^2$	$c \times 10^2$	$c_e \times 10^2$
STEPPED	- 6.47	1.09	0.25
r/D = 1/2	- 2.04	1.43	0.59
θ = 30°	- 0.32	0.84	0
SQUARE	- 2.88	1.63	0.79
r/D = 1/8	- 3.17	1.75	0.91
θ = 90°	- 6.96	2.67	1.83
θ = 60°	- 5.19	2.45	1.61
r/D = 1/4	- 2.42	2.11	1.27
r/D = 3/8	- 8.46	2.82	1.98
r/D = 1/2	- 5.90	1.87	1.03
BULLET	- 2.31	1.43	0.59

$$\zeta = b + cV , \quad \text{for} \quad 6.1 \, m/s < V < 16.8 \, m/s$$

3. <u>Multiple Cylinders in Axial Flow</u>

When an array of N cylinders is subjected to axial flow, fluid damping consists of three parts: viscous damping, Coriolis force, and drag force. This is the same as for a single cylinder. However, multiple cylinders include coupling effect. The damping coefficients can be written as follows:

$$\alpha'_{ij} = \alpha'_{oij} + 2V\alpha_{ij}\frac{\partial}{\partial z} + \alpha'_{dij} \; ,$$

$$\sigma'_{ij} = \sigma'_{oij} + 2V\sigma_{ij}\frac{\partial}{\partial z} + \sigma'_{dij} \; ,$$

$$(46)$$

$$\tau'_{ij} = \tau'_{oij} + 2V\tau_{ij}\frac{\partial}{\partial z} + \tau'_{dij} \; ,$$

and

$$\beta'_{ij} = \beta'_{oij} + 2V\beta_{ij}\frac{\partial}{\partial z} + \beta'_{dij} \; .$$

The first terms are the viscous damping coefficients in stationary fluid, the second terms are associated with the Coriolis force, and the third terms are drag-induced damping coefficients.

At present, these coefficients are not available for arbitrary cylinder arrays. The viscous damping coefficients in stationary fluid, α'_{oij}, σ'_{oij}, τ'_{oij}, and β'_{oij} can be obtained using a finite element technique [9]. The coefficients in the Coriolis force terms are those of added mass, which can be calculated using the potential flow theory [2] or linearized viscous flow theory [9]. The drag coefficients are not well understood. Paidoussis and Suss proposed a method of solution based on the potential flow solution but the results have not been verified [36].

The damping of an uncoupled mode of a 3 x 3 array of 6.35-mm (0.25-in.) diameter rods with an effective length of 0.495 m (19.5 in.) between simple supports has been reported [37]. The rods are arranged in a square pattern with a pitch-to-diameter ratio of 1.33. The modal damping ratio is given by

$$\zeta_1 = 1.71 \left(\frac{\rho D^2}{m + m_f}\right) \left(\frac{\nu}{f_n D^2}\right)^{0.5} \exp\left(-0.00018 \frac{DV}{\nu}\right)$$

$$+ 0.052 \left(\frac{\rho D^2}{m + m_f}\right) \left(\frac{V}{f_n D}\right) \left(\frac{\nu}{DV}\right)^{0.22} , \qquad (47)$$

where f_n = natural frequency, D = rod diameter, $m + m_f$ = effective mass per unit length, ν = kinetic viscosity, ρ = fluid density, and V = flow velocity. The first term in Eq. 47 is the viscous damping in quiescent fluid and the second is the damping induced by drag force. Because the rods are supported at both ends, the damping associated with the Coriolis force is zero.

Further investigations are needed to quantify the fluid damping for cylinder arrays in axial flow.

4. Cylindrical Shells Conveying Fluid

The fluid damping for a cylindrical shell conveying fluid also is important. Most studies are based on the linearized, unsteady potential flow theory [38-41]. The analysis for this problem is quite involved. It is difficult to present fluid damping for general applications. For a specific problem, a detailed study would have to be performed for each case.

V. CROSSFLOW

1. A Single Cylinder Subjected to Crossflow

The mathematical representation of a single cylinder in crossflow is very complicated. If the motion of the cylinder is small with respect to the approaching flow, the flow-velocity-dependent damping force can be represented by [42,43] (see Fig. 17)

$$f = \rho V D C_D \frac{\partial u}{\partial t}$$

and   (48)

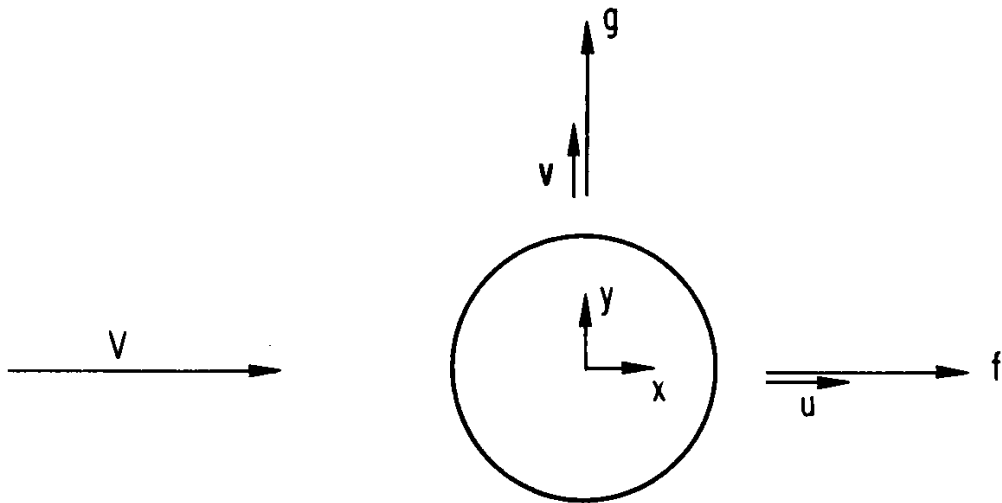$$g = \frac{1}{2} \rho V D C_D \frac{\partial v}{\partial t} ,$$

Fig. 17. A single cylinder subjected to crossflow.

where C_D is the drag coefficient. The modal damping ratios in the x and y directions are

$$\zeta_x = \frac{C_D}{\pi^2} \left(\frac{M_d}{m + M_d}\right) \left(\frac{V}{f_n D}\right)$$

and (49)

$$\zeta_y = \frac{C_D}{2\pi^2} \left(\frac{M_d}{m + M_d}\right) \left(\frac{V}{f_n D}\right) ,$$

where f_n is the natural frequency of the cylinder in cycles per second.

Experimental data obtained in water for low reduced-flow velocity ($V/f_n D < 5$) are given in Figs. 18 and 19 in the lift and drag directions [43]. The resultant damping is given; the flow-velocity dependent damping may be obtained by subtracting the damping value at zero flow velocity. The Reynolds number ranges from 10^3 to 5×10^4 in Figs. 18 and 19. The steady state drag coefficient is about 1. Based on the steady state drag, the modal damping calculated from Eqs. 49 will be larger than the experimental results given in Figs. 18 and 19. Therefore, the drag coefficient for steady flow cannot be applied to this case, in which the steady flow is superimposed with a pulsating component. Based on the results of Figs. 18 and 19, the values of drag coefficient are 0.35 and 0.19, respectively.

In the "synchronization region," in which cylinder motion is locked in to vortex shedding process, flow/cylinder interaction becomes important. Equation 49 is no longer applicable in this region. Damping ratios in the lift direction for a system in wind tunnel are shown in Fig. 20 for reduced flow velocity ($V/f_n D$) from 0 to 20 and Reynolds number from 300-1000 [44]. Damping changes slowly at low flow velocity and then decreases to a minimum value as the velocity increases within the resonant range. The minimum range of damping occurs near the maximum amplitude of the cross-flow vibration, and damping begins to increase thereafter. Above the lock-in range, the damping increases more rapidly with flow.

Based on these results, it appears that for a single cylinder, Eq. 49 can be applied to obtain fluid damping outside the lock-in range, although the value of the drag coefficient for steady flow cannot be used. In the
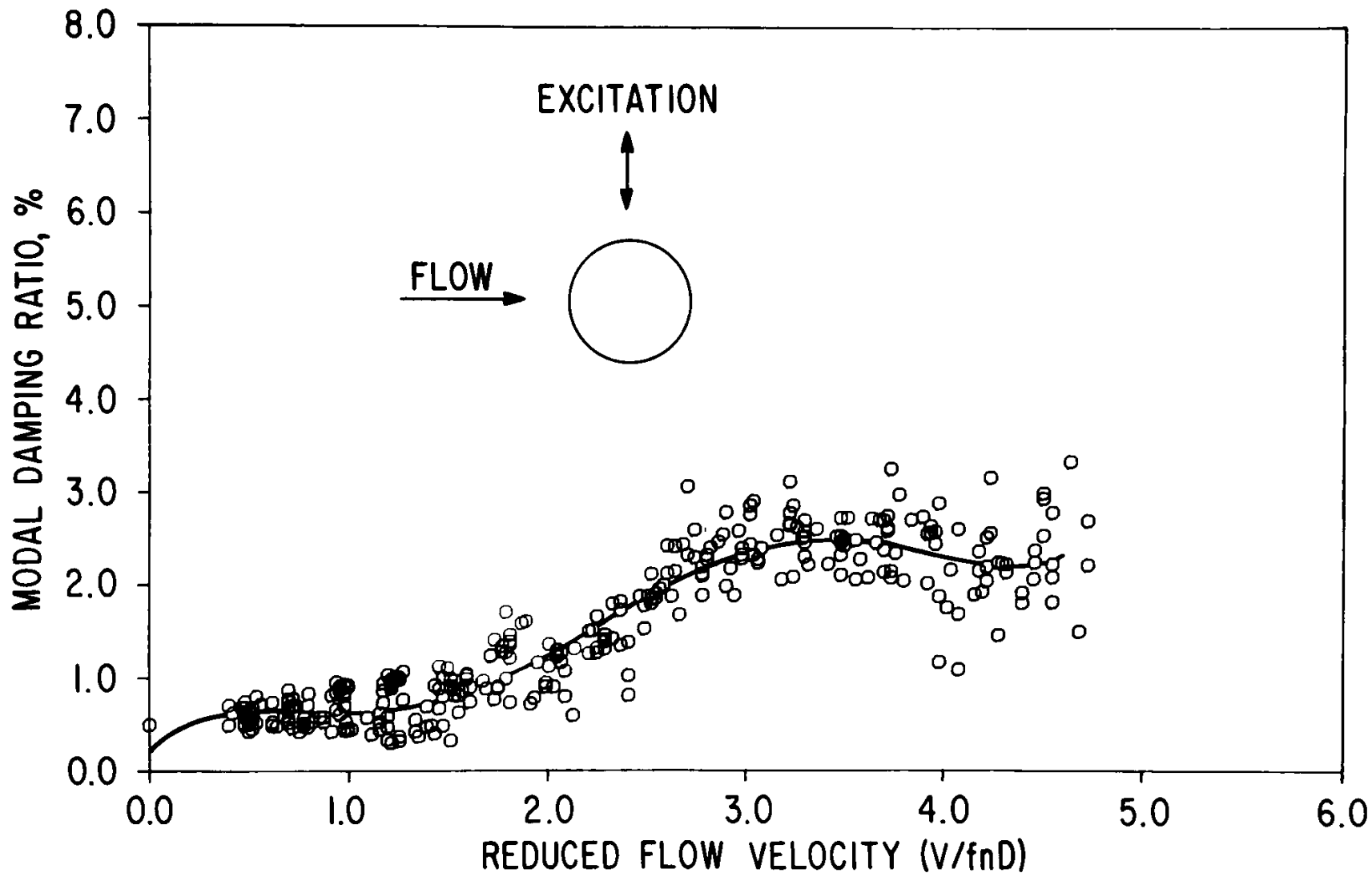
Fig. 18. Modal damping ratio in the lift direction [Ref. 43].
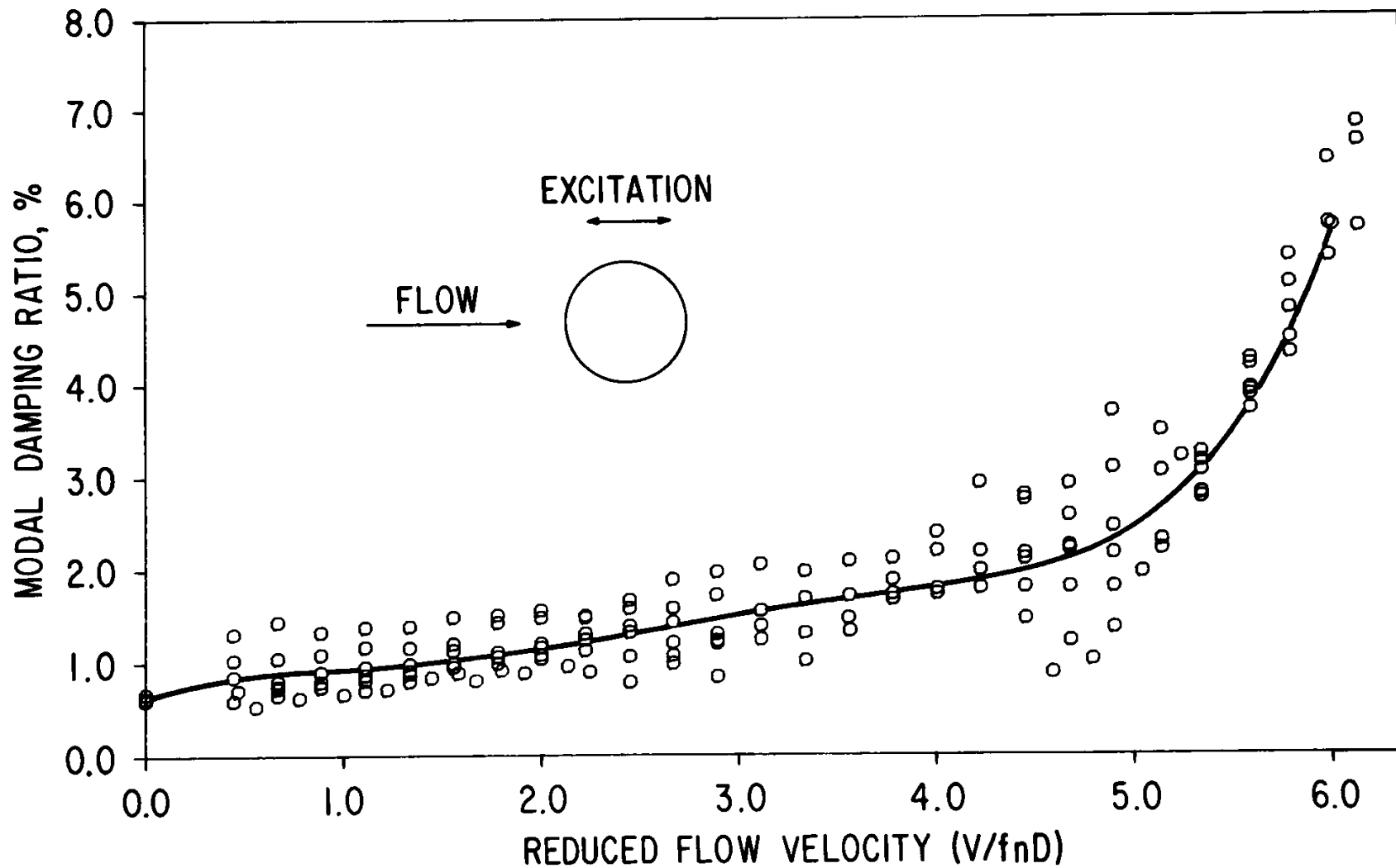
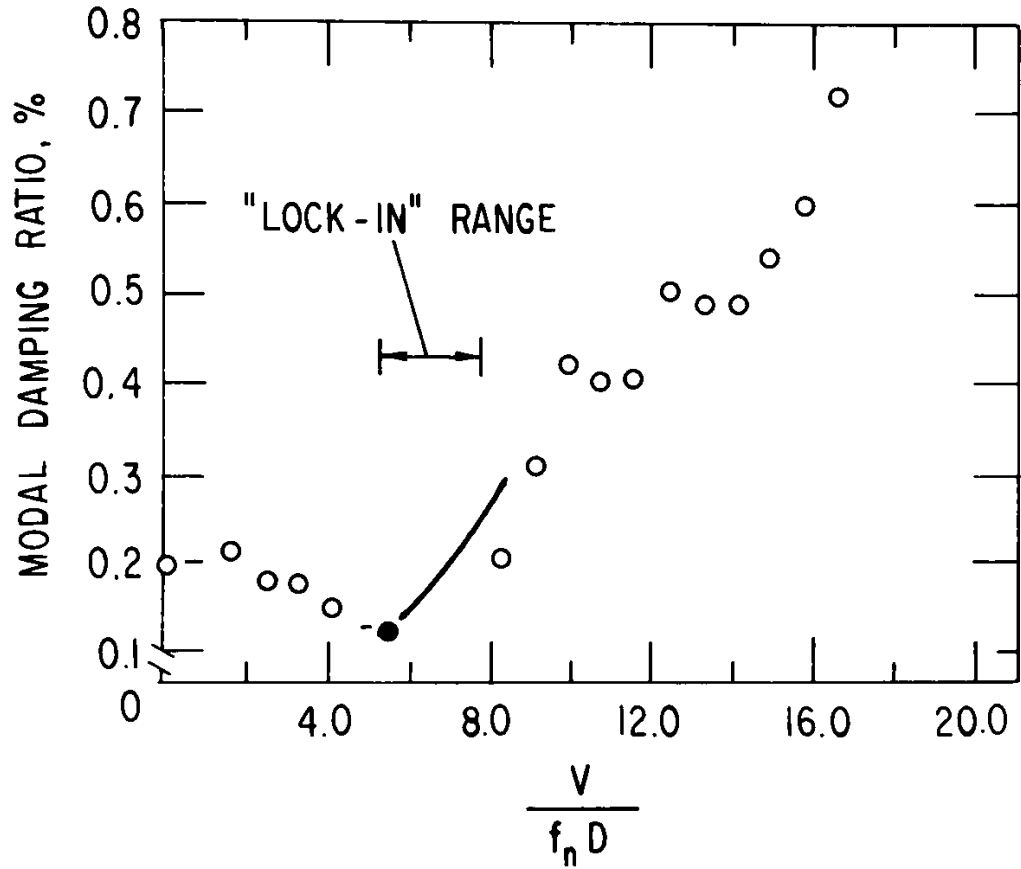Fig. 19. Modal damping ratio in the drag direction [Ref. 43].

Fig. 20. Modal damping ratio in the lift direction [Ref. 44].

lock-in region, representation of fluid damping is still difficult; the results given in Fig. 20 actually are a manifestation of the coupling between vortex shedding and cylinder motion.

The drag coefficient for an oscillating cylinder in crossflow has been measured directly by Souders et al. [45]. The drag coefficient is found to depend on the cylinder oscillation amplitude, Reynolds number, and ratio of forced oscillation frequency to Strouhal frequency. Figures 21 and 22 show the variation of drag and lift coefficients as a function of frequency ratio for different vibration amplitude; C_D is in general greater than that for a non-oscillating cylinder, and approximately independent of S_f/S_n for $S_f/S_n >$ about 0.4. For $S_f/S_n < 0.4$, C_D is basically the same as for the non-oscillating cylinder. The effect of Reynolds number on C_D seems to decrease as the vibration amplitude increases.

The lift coefficient given in Fig. 22 shows that for the smaller values of oscillation amplitude and S_f/S_n, the lift coefficient decreases with increasing Re. For larger values of oscillation amplitudes and S_f/S_n, C_L is not sensitive to Re.

Most recently, Kato et al. [46] have systematically studied the drag force on oscillating cylinders in a uniform flow. The drag coefficient C_D is a function of reduced flow velocity V/f_nD and Keleugan-Carpenter parameter K_c. In general the drag coefficient increases with U/f_nD and K_c. More measurements are needed to determine the value of the drag and lift coefficients for a cylinder oscillating in a flow.

2. A Pair of Cylinders in Crossflow

The flow field around a pair of circular cylinders is very complex and has been studied extensively [47]. However, there is very limited information on damping. A complete description of the damping characteristics requires the knowledge of α'_{ij}, σ'_{ij}, τ'_{ij}, and β'_{ij} in Eq. 1. At present, no such information is available for a pair of cylinders.

Modal damping for two cylinders normal to a flow was measured by Jendrzejczyk et al. [48]. The modal damping for a particular mode is given in Fig. 23. Those damping values correspond to the out-of-phase mode of in-plane motion. Note that damping increases with flow at small flow
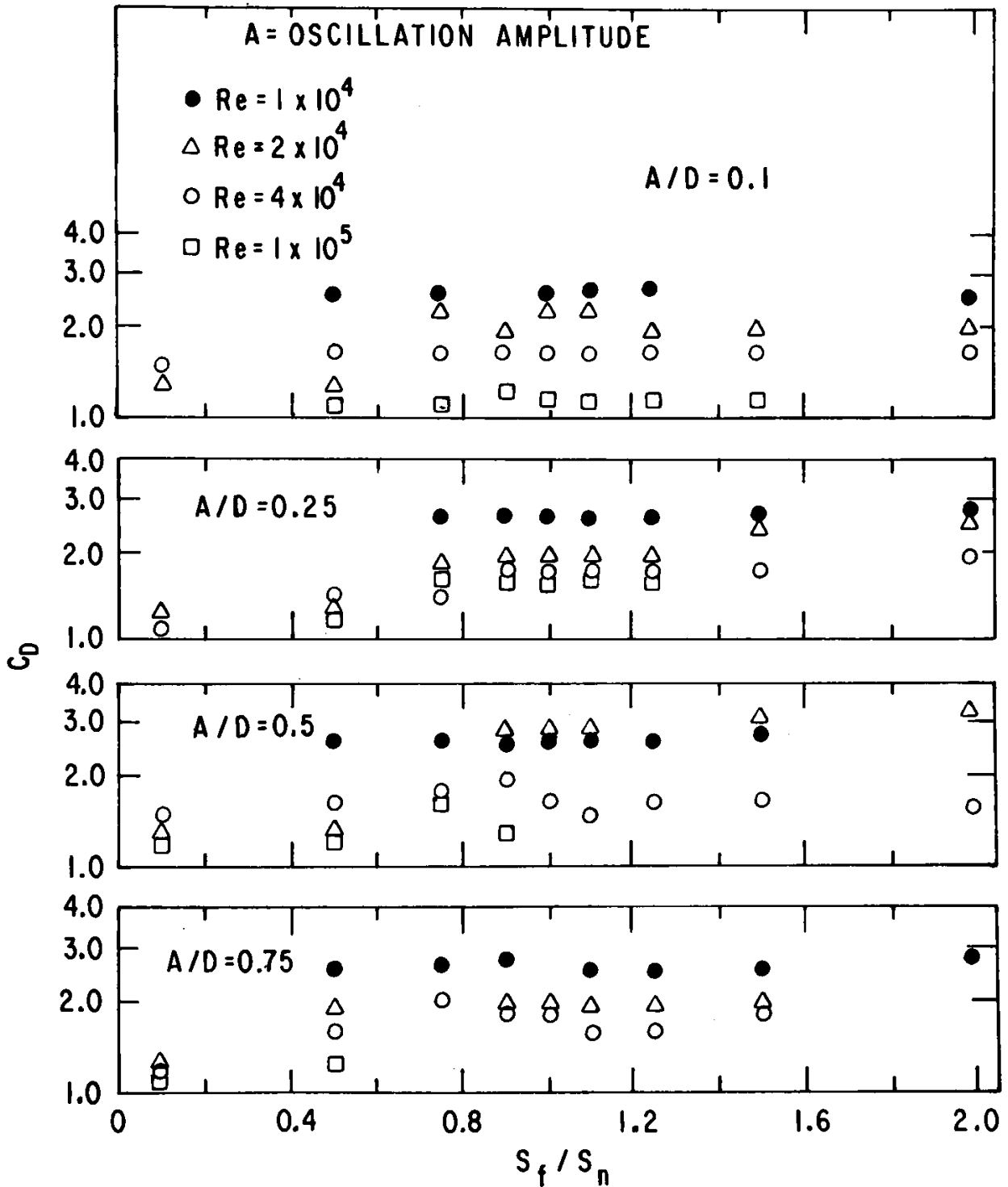
Fig. 21. Variation of drag coefficient as function of the ratio of forced to natural Strouhal numbers [Ref. 45].
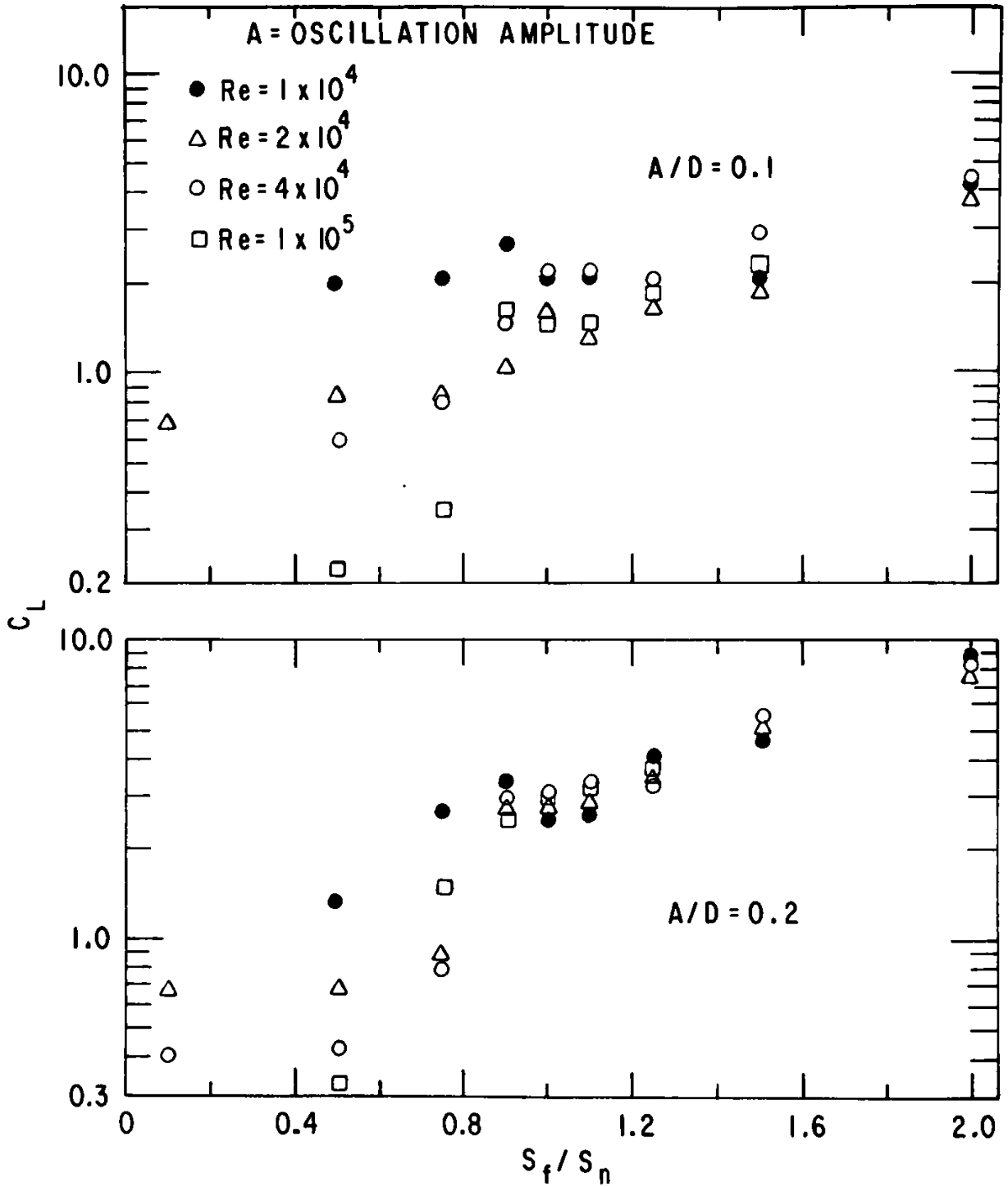
Fig. 22. Variation of lift coefficient as function of the ratio of forced
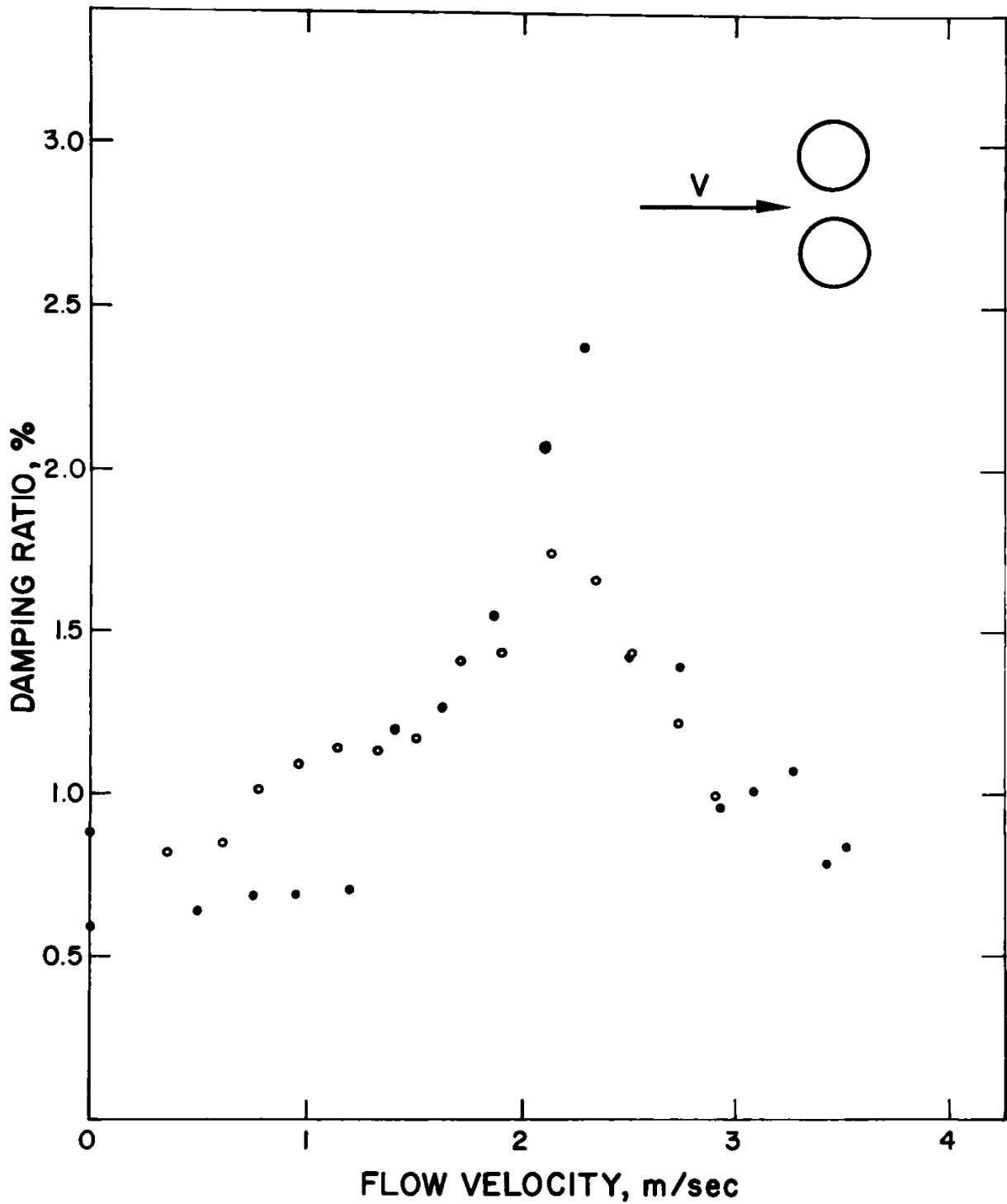to natural Strouhal numbers [Ref. 45].

Fig. 23. Modal damping ratio in the lift direction for two tubes normal
to a flow [Ref. 48].

velocities. It reaches a peak at a flow velocity approximately equal to that associated with the maximum cylinder displacement in the drag direction, a velocity at which tube motion in the drag direction synchronizes with vortex shedding. With further increase in flow velocity, damping decreases with flow velocity.

The aerodynamic forces acting on twin circular conductors have been considered in the study of "wake-induced flutter" [49]. The fluid damping forces depend on conductor spacing and conductor arrangement. In general, detailed measurements have to be performed to quantify the amplitude of fluid forces. It is not possible, at present, to present a simple design guide for this problem.

3. A Group of Cylinders in Crossflow

As in the case of two cylinders, no complete data on α'_{ij}, σ'_{ij}, τ'_{ij}, and β'_{ij} are available. There are only a few studies directed to obtain the damping for tube arrays [50-52].

Two tube arrays, as shown in Figs. 24, were tested by Chen and Jendrzejczyk [50]: (1) In-line array with longitudinal pitch P/D = 1.5 and transverse pitch T/D = 1.5 and (2) Staggered array with P/D = 1.5, and T/D = 1.6. Damping was measured for the active tubes, located at positions 1, 2, and 3, in both lift and drag directions. The measured damping corresponds to the contribution from the diagonal terms of α'_{ij} and β'_{ij}.

Two typical results are given in Figs. 25 and 26; the total damping is presented for all tests. The flow velocity-dependent damping can be obtained by subtracting the damping at zero flow from the total damping.

Based on the experimental results, general trends of the flow velocity-dependent damping for tube arrays are given in Fig. 27 in the drag and lift directions for $V/f_nD < 10$. In general, V_1 corresponds to the beginning of synchronization of vortex shedding with tube natural frequency; V_2 corresponds to the coincidence of vortex shedding and tube natural frequencies; and V_3 corresponds to the decrease of damping again in the lift direction. General characteristics of damping in tube arrays are similar to those of a single tube. However, in cylinder arrays, flow velocity-dependent damping may change from dissipating energy to causing instability.
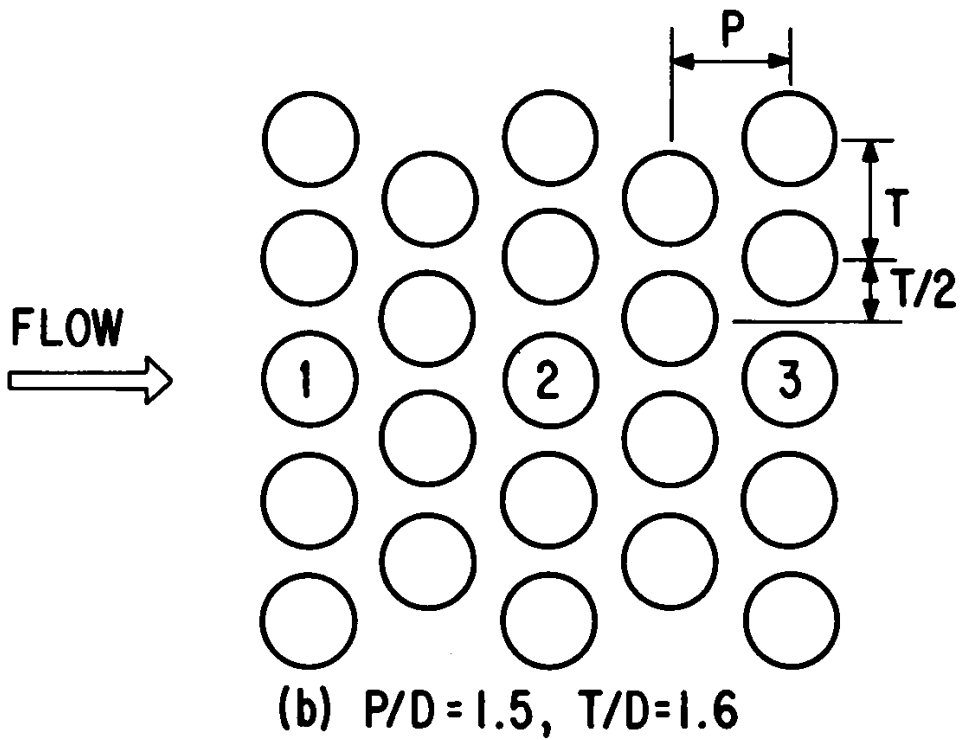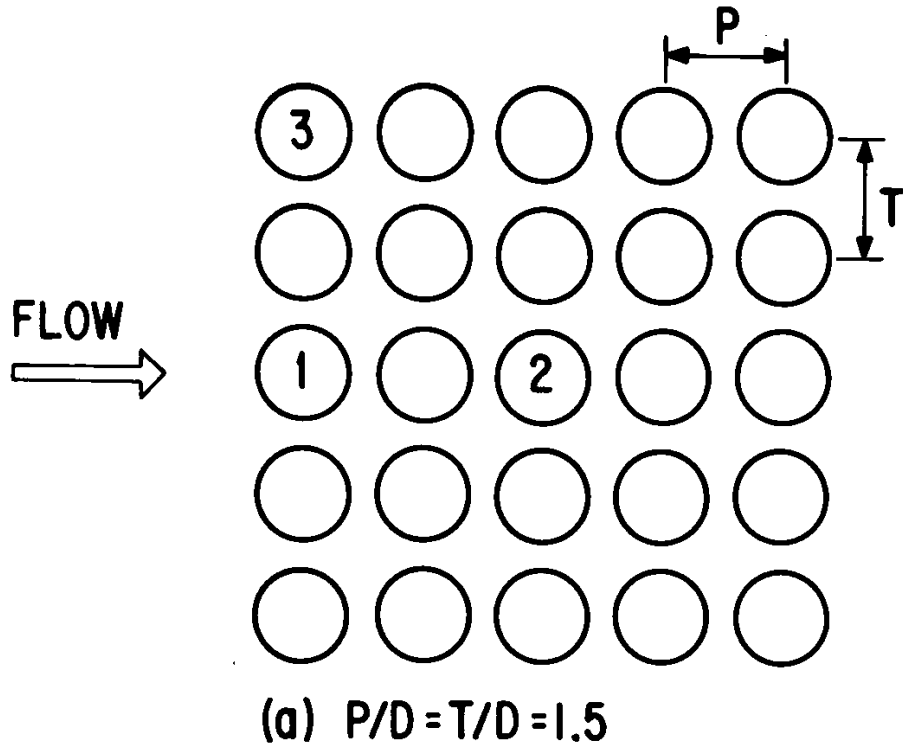
Fig. 24.   Two tube array.
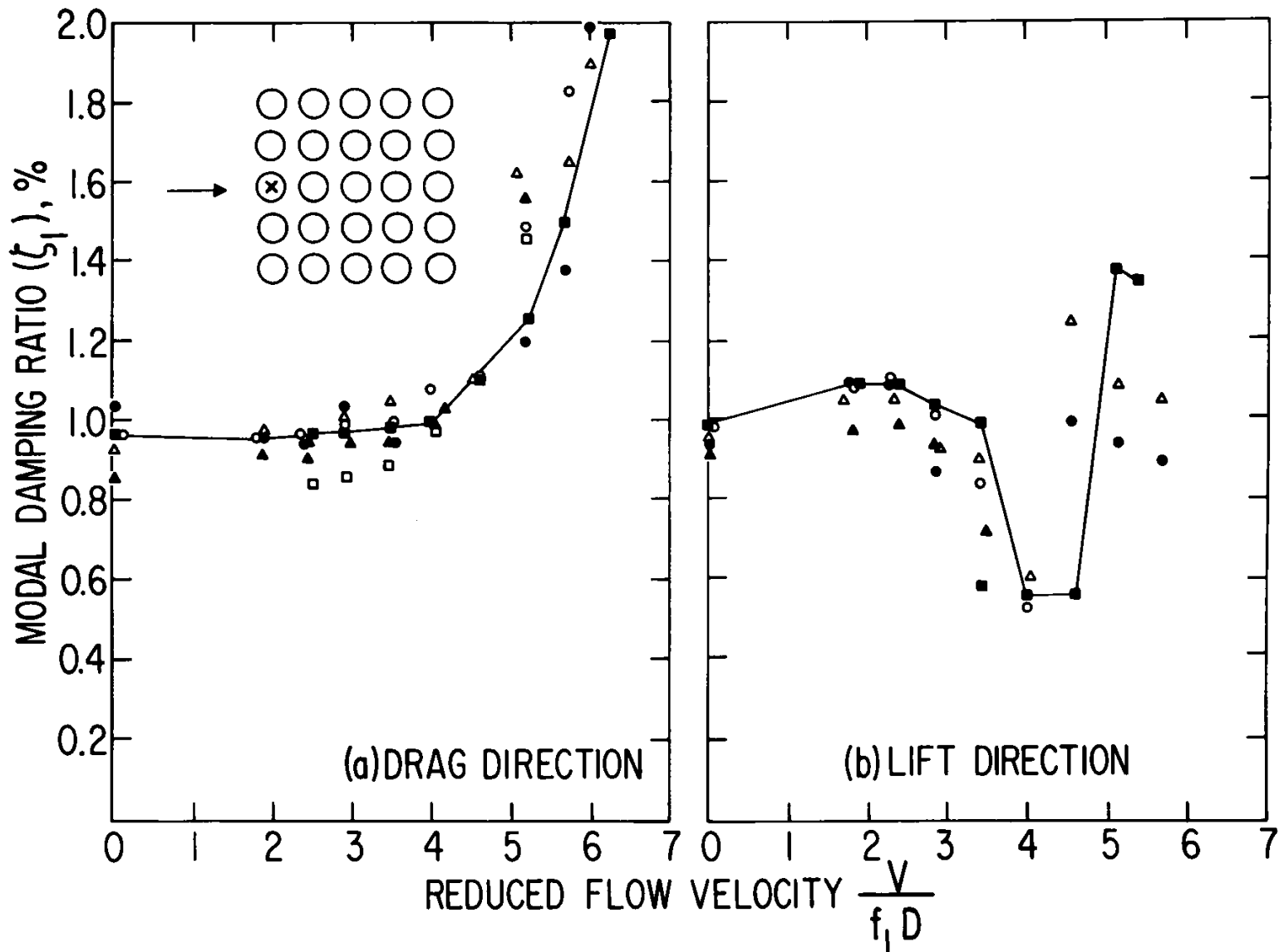
Fig. 25. Modal damping ratio for a tube in a square array [Ref. 50].
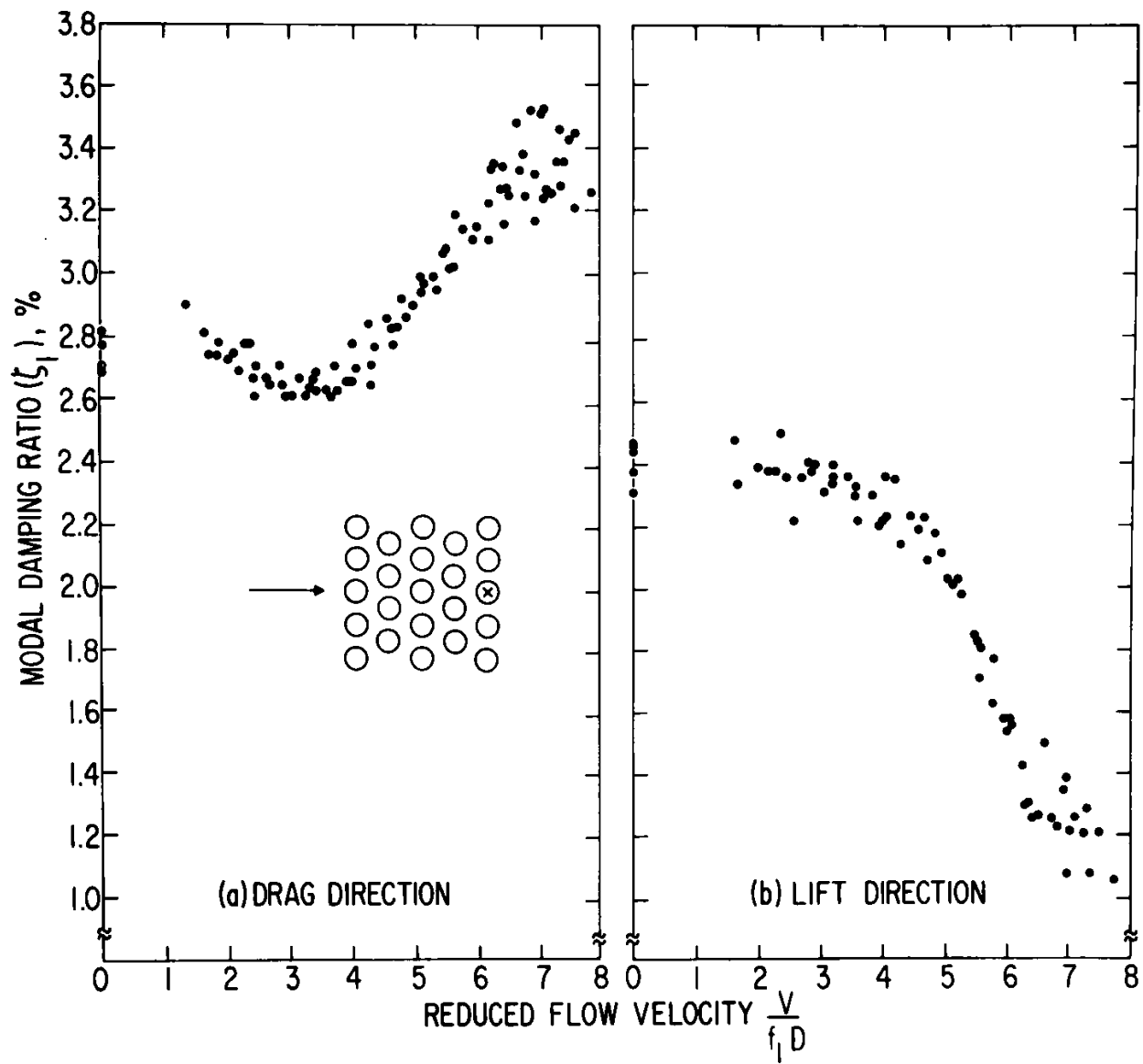
Fig. 26. Modal damping ratio for a tube in a staggered array [Ref. 50].

64
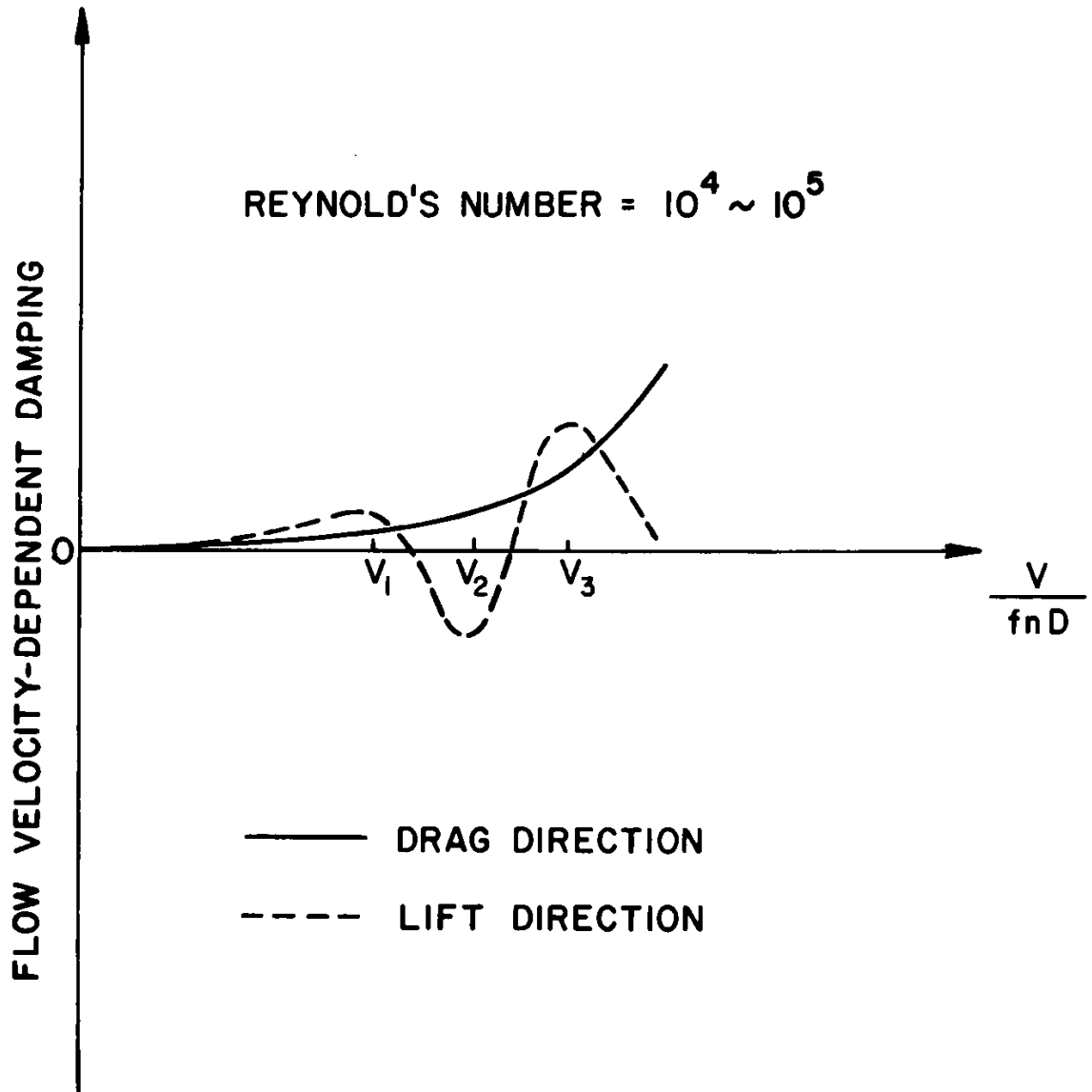
Fig. 27. General trends of flow-velocity-dependent damping for tube arrays
[Ref. 50].

The fluid force components acting on tube arrays are measured and reported by Tanaka and his colleagues for a row of tubes and a square array, both with a pitch-to-diameter ratio of 1.33, as shown in Fig. 28 [51,52]. In addition, the fluid forces for a square array with a pitch-to-diameter ratio of 2.0 also are measured [53]. From these data, fluid-damping coefficients can be calculated. Tables 3, 4, and 5 show the fluid-damping coefficients $\bar{\alpha}'_{ij}$, $\bar{\beta}'_{ij}$, $\bar{\sigma}'_{ij}$, and $\bar{\tau}'_{ij}$; these coefficients are defined as follows:

$$\bar{\alpha}'_{ij} = \left(\frac{\omega}{\rho V^2}\right) \alpha'_{ij} \ ,$$

$$\bar{\beta}'_{ij} = \left(\frac{\omega}{\rho V^2}\right) \beta'_{ij} \ ,$$

$$\bar{\sigma}'_{ij} = \left(\frac{\omega}{\rho V^2}\right) \sigma'_{ij} \ ,$$

and

$$\bar{\tau}'_{ij} = \left(\frac{\omega}{\rho V^2}\right) \tau'_{ij} \ .$$

(50)

Note that Eq. 50 is applicable for reduced flow velocity U_f not equal to zero only. The coefficients depend on the reduced flow velocity U_f. For larger values of U_f, the absolute values of these coefficients are approximately constants.

VI. EXAMPLES OF APPLICATION

Consider a simply supported tube with a baffle plate at midspan (see Fig. 29). The tube is a stainless tube submerged in water (70°F). Tube properties are given as follows:

Tube O.D. (2r) = 1 in.,

Tube wall thickness = 1/8 in.,

Tube length ℓ = 48 in.,
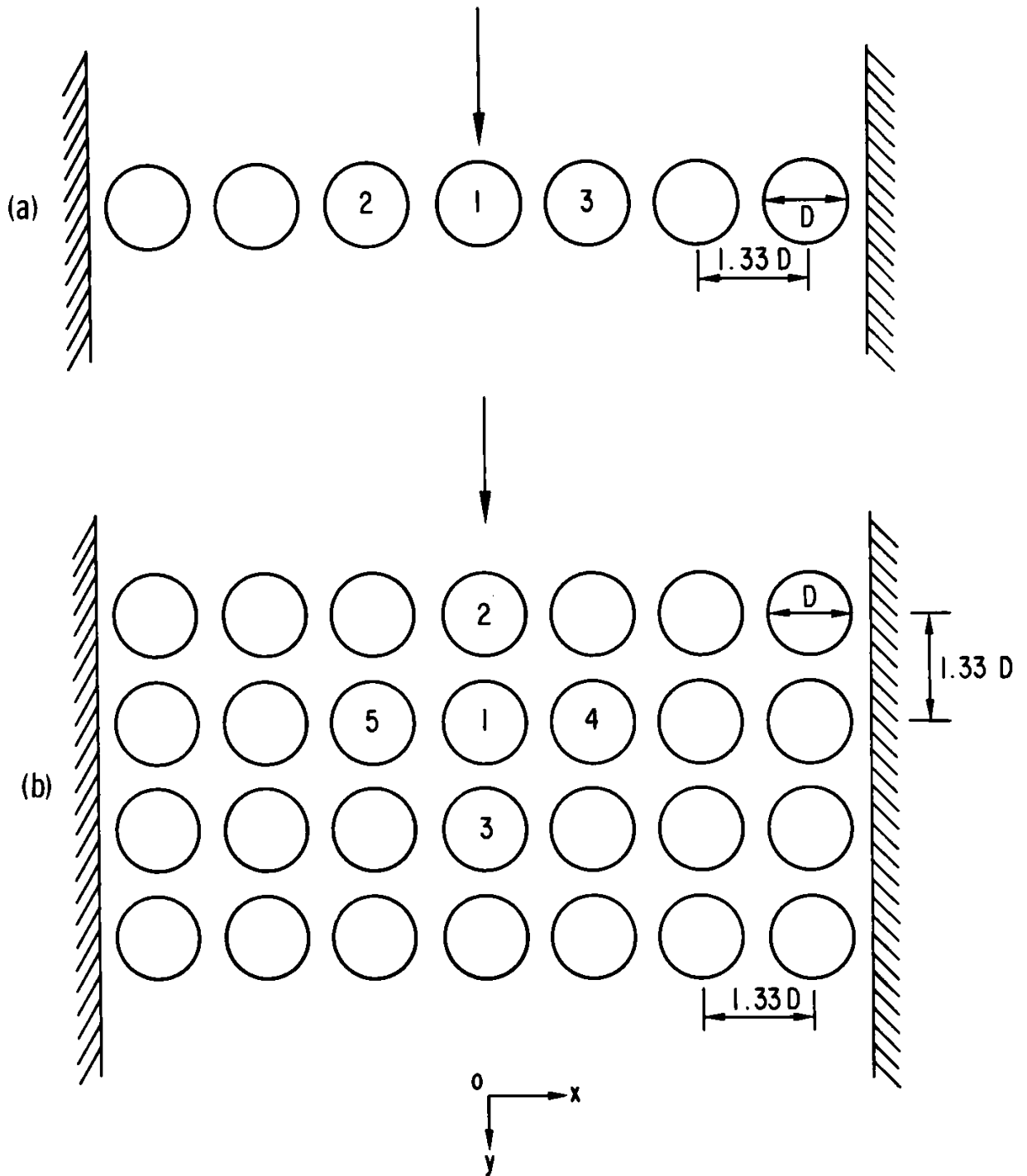
Fig. 28.   A row of cylinders and a square array.

Table 3. Fluid-damping coefficients for a tube row with P/D = 1.33

U_f	$\bar{\alpha}'_{11}$	$\bar{\alpha}'_{12}$	$\bar{\sigma}'_{12}$	$\bar{\beta}'_{11}$	$\bar{\tau}'_{12}$	$\bar{\beta}'_{12}$
1.5	0.0	0.167	-2.228	0.524	-0.804	0.0
2.0	-0.297	0.141	-1.167	0.297	-0.611	0.209
3.0	-0.349	0.282	-0.667	0.543	-0.344	0.525
4.0	-0.956	0.498	-0.206	0.679	-0.373	0.546
5.0	-1.256	0.536	0.000	0.537	-0.394	0.441
6.0	-0.994	0.246	0.079	0.469	-0.379	0.354
7.0	-0.656	0.063	0.106	0.471	-0.330	0.290
8.0	-0.338	-0.022	0.130	0.468	-0.275	0.248
9.0	-0.052	-0.059	0.129	0.446	-0.230	0.216
10.0	0.079	-0.076	0.099	0.423	-0.205	0.188
15.0	0.225	-0.103	0.062	0.240	-0.136	0.126
20.0	0.229	-0.095	0.056	0.146	-0.065	0.082
30.0	0.202	-0.088	0.046	0.102	-0.038	0.028
40.0	0.175	-0.078	0.038	0.094	-0.030	0.016
50.0	0.153	-0.074	0.038	0.091	-0.026	0.014
60.0	0.141	-0.069	0.034	0.088	-0.022	0.009
70.0	0.135	-0.064	0.031	0.085	-0.020	0.007
80.0	0.129	-0.060	0.031	0.085	-0.018	0.007
90.0	0.126	-0.057	0.032	0.083	-0.016	0.004
100.0	0.123	-0.054	0.037	0.091	-0.018	0.004

Table 4. Fluid-damping coefficients for a square array with P/D = 1.33

U_f	$\bar{\alpha}'_{11}$	$\bar{\alpha}'_{12}$	$\bar{\alpha}'_{13}$	$\bar{\alpha}'_{14}$	$\bar{\beta}'_{11}$	$\bar{\beta}'_{12}$	$\bar{\beta}'_{13}$	$\bar{\beta}'_{14}$	$\bar{\sigma}'_{15}$	$\bar{\tau}'_{15}$
1.500	1.021	−0.471	0.564	0.549	0.994	0.557	−0.414	−0.092	−2.561	−0.933
2.000	0.604	−0.521	0.544	0.469	1.124	0.439	−0.272	−0.103	−1.682	−1.205
2.500	0.853	−0.524	0.549	0.518	1.406	0.401	−0.209	−0.131	−1.303	−1.269
3.000	0.350	−0.539	0.556	0.524	1.465	0.381	−0.412	−0.090	−0.919	−1.141
3.500	0.0	−0.517	0.602	0.559	1.245	0.390	−0.324	0.268	−0.602	−0.940
4.000	−0.061	−0.485	0.667	0.552	1.320	0.082	−0.323	0.496	−0.356	−0.834
5.000	−0.101	−0.359	0.679	0.461	1.166	−0.305	−0.355	0.594	−0.042	−0.685
6.000	−0.149	−0.249	0.638	0.408	1.031	−0.340	−0.357	0.495	0.082	−0.593
7.000	−0.162	−0.179	0.606	0.352	0.901	−0.220	−0.335	0.423	0.135	−0.531
8.000	−0.159	−0.103	0.598	0.272	0.818	−0.144	−0.283	0.376	0.138	−0.481
10.000	−0.169	−0.026	0.587	0.082	0.671	−0.108	−0.231	0.324	0.124	−0.429
12.000	−0.094	0.010	0.493	−0.010	0.552	−0.092	−0.222	0.310	0.117	−0.402
15.000	−0.103	0.037	0.409	−0.043	0.457	−0.072	−0.218	0.310	0.109	−0.374
20.000	−0.125	0.061	0.333	−0.060	0.385	−0.062	−0.195	0.307	0.100	−0.334
25.000	−0.153	0.070	0.293	−0.047	0.329	−0.056	−0.175	0.293	0.101	−0.301
30.000	−0.179	0.080	0.265	−0.039	0.292	−0.051	−0.151	0.280	0.096	−0.271
35.000	−0.197	0.067	0.246	−0.061	0.254	−0.046	−0.136	0.249	0.089	−0.245
40.000	−0.211	0.094	0.246	−0.093	0.221	−0.045	−0.113	0.201	0.078	−0.227
50.000	−0.215	0.100	0.246	−0.129	0.167	−0.040	−0.088	0.156	0.059	−0.201
60.000	−0.206	0.093	0.247	−0.159	0.138	−0.035	−0.066	0.156	0.036	−0.187
80.000	−0.181	0.073	0.240	−0.195	0.091	−0.029	−0.032	0.176	−0.009	−0.173
100.00	−0.154	0.063	0.236	−0.200	0.063	−0.023	−0.022	0.190	−0.060	−0.168

Table 5. Fluid-damping coefficients for a square array with $P/D = 2.0$

| U_f	$\bar{\alpha}'_{11}$	$\bar{\alpha}'_{12}$	$\bar{\alpha}'_{13}$	$\bar{\alpha}'_{14}$	$\bar{\beta}'_{11}$	$\bar{\beta}'_{12}$	$\bar{\beta}'_{13}$	$\bar{\beta}'_{14}$	$\bar{\sigma}'_{15}$	$\bar{\tau}'_{15}$
6.000	−0.820	0.116	0.100	−0.056	0.514	0.525	−0.095	0.373	−0.108	−0.138
8.000	−0.797	0.247	0.010	−0.127	0.371	0.249	−0.097	0.249	0.050	−0.155
10.000	−0.486	0.189	0.007	−0.077	0.287	0.124	−0.089	0.177	0.044	−0.127
15.000	−0.314	0.267	0.009	−0.043	0.186	−0.062	−0.064	0.102	0.010	−0.085
20.000	−0.288	0.271	0.009	−0.029	0.140	−0.062	−0.046	0.073	−0.002	−0.065
30.000	−0.249	0.249	0.009	−0.019	0.095	−0.029	−0.018	0.049	−0.015	−0.049
40.000	−0.219	0.224	0.008	−0.011	0.074	−0.018	0.003	0.036	−0.019	−0.042
50.000	−0.189	0.192	0.007	−0.006	0.057	−0.009	0.010	0.029	−0.015	−0.035
70.000	−0.143	0.140	0.005	−0.001	0.046	−0.001	0.002	0.020	−0.019	−0.035
100.00	−0.119	0.098	0.002	0.001	0.039	−0.000	−0.008	0.016	−0.001	−0.033

69
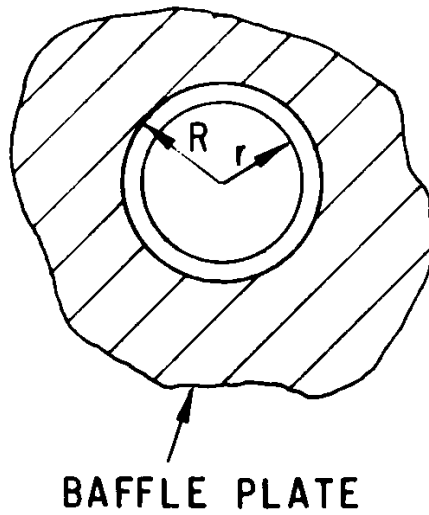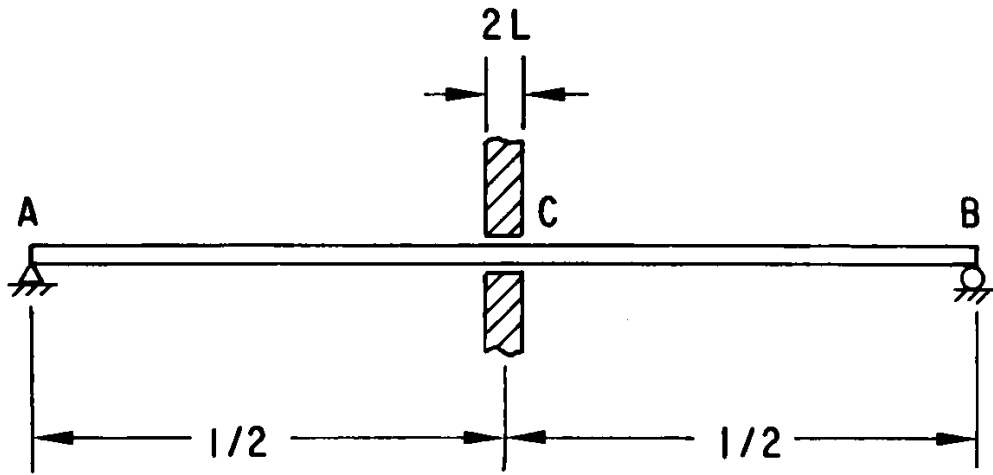
Fig. 29. A simply-supported tube with a baffle-plate support.

Baffle-plate-hole diameter (2R) = 1.02 in.,

Baffle plate thickness (2L) = 1.5 in.

We wish to calculate the fluid damping with and without the baffle plate.

(a) <u>No Baffle Plate</u>

For the case of a tube vibrating in an infinite fluid, the modal damping ratio attributed to fluid can be calculated from Eq. 10:

$$\zeta_n = -\frac{1}{2}\left(\frac{M_d}{C_M M_d + m}\right)\text{Im}(H) \ . \tag{51}$$

Note that the natural frequency of the fundamental mode is given by

$$\omega_1 = \frac{\pi^2}{\ell^2}\left(\frac{EI}{C_M M_d + m}\right)^{0.5} \ , \tag{52}$$

and that

$$E = 30 \times 10^6 \text{ lb/in. } ,$$

$$I = \frac{\pi}{64}(1.0^4 - 0.75^4)\text{in.}^4 = 0.0336 \text{ in.}^4 \ , \tag{53}$$

$$m = \frac{\pi}{4}(1^2 - 0.75^2)\cdot 7.5 \times 10^{-4} \text{ lb-sec}^2/\text{in.}^2 = 2.58 \times 10^{-4} \text{ lb-sec}^2/\text{in.}^2,$$

and

$$M_d = \frac{\pi}{4} \times 0.935 \times 10^{-4} \times 1.0^2 \text{ lb-sec}^2/\text{in.}^2 = 0.734 \times 10^{-4} \text{ lb-sec}^2/\text{in.}^2$$

The effect of fluid viscosity on C_M is small; C_M is assumed to be 1. Substituting these values into Eq. 52 yields

$$\omega_1 = 236.3 \text{ rad/sec}$$

and

$$S = \frac{\omega_1 r^2}{\nu} = \frac{236.3 \times 1^2}{0.00157} = 1.5 \times 10^5 \ .$$

From Fig. 5, Re(H) $\simeq$ 1 and $-\text{Im}(H) = 0.0075$. Therefore,

$$\zeta_1 = \frac{1}{2}\left(\frac{0.734}{0.734 + 2.58}\right) \times 0.0075 = 0.083\% \ .$$

The modal damping attributed to fluid is small.

    (b) With Baffle Plate

        The equation of motion of the tube is given as follows:

$$EI \frac{\partial^4 u}{\partial z^4} + \bar{C}_v \delta \left(\frac{\ell}{2}\right) \frac{\partial u}{\partial t} + (m + C_M M_d) \frac{\partial^2 u}{\partial t^2} = 0 \ , \tag{54}$$

where EI = flexural rigidity, u = tube displacement, t = time, δ = delta function, m = tube mass per unit length, and $C_M M_d$ = added mass per unit length. The second term is the damping associated with the fluid in the annular region of the baffle plate; all other damping and excitation forces are neglected in Eq. 54. Since the tube is hinged at both ends, let

$$u = q(t)\sin \frac{n \pi x}{\ell} \ . \tag{55}$$

Using Eqs. 54 and 55 yields

$$\frac{d^2 q}{dt^2} + 2 \zeta_n \omega_n \frac{dq}{dt} + \omega_n^2 q = 0 \ ,$$

$$\omega_n = \frac{n^2 \pi^2}{\ell^2} \left(\frac{EI}{m + C_M M_d}\right)^{0.5} \ ,$$

$$\tag{56}$$

$$\zeta_n = \frac{\bar{C}_v}{(m + C_D M_D) \ell \omega_n} \ , \qquad n = odd$$

$$= 0 \ , \qquad\qquad n = even \ .$$

The damping coefficient $\bar{C}_v$ is given by

$$\bar{C}_v = \int_{-L}^{L} C_v dz \ , \tag{57}$$

where C_v is given in Eq. 11,

$$C_v = -M_d \left(\frac{r}{R-r}\right) \omega_n \text{Im}(H) \left[1 - \frac{\cosh(z/R)}{\cosh(L/R)}\right] . \tag{58}$$

Substituting Eq. 58 into 57 yields

$$\bar{C}_v = 2LKM_d \left(\frac{r}{R-r}\right) \omega_n [-\text{Im}(H)]$$

and $\qquad\qquad$ (59)

$$K = 1 - \frac{r}{L} \tanh \left(\frac{L}{r}\right) .$$

Substituting Eq. 59 into 56 yields

$$\zeta_n = KM_d \left(\frac{r}{R-r}\right)[-\text{Im}(H)] \frac{2L}{(m + C_D M_D)\ell} , \quad n = \text{odd}$$

$$= 0 , \qquad\qquad\qquad n = \text{even} . \tag{60}$$

When n is an odd number, the tube vibrates within the gap (see Fig. 30); the fluid in the annular contributes to damping. When n is even, the tube vibrates against the baffle plate, the midspan at the baffle plate is a nodal point and the damping attributed to the fluid at the baffle plate is zero.

In Eq. 60, the function H depends on the oscillation frequency; therefore, the modal damping for different modes are different. Based on Eq. 60 and Fig. 7 the modal damping for the fundamental mode is calculated as follows:

$$\frac{1}{R-r} \sqrt{\frac{2\nu}{\omega_1}} = \frac{1}{0.01} \left(\frac{2 \times 0.00157}{236.3}\right)^{0.5} = 0.365 .$$

From Fig. 7, $-\text{Im}(H) = 0.82$,

(I) TUBE VIBRATING WITHIN THE GAP
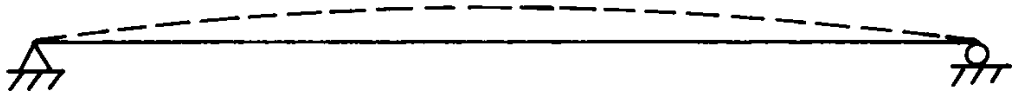
(2) TUBE VIBRATING AGAINST THE GAP

Fig. 30. Different modes for a tube with motion-limiting gap.

$$K = 1 - \frac{r}{L} \tanh \left(\frac{L}{r}\right)$$

$$= 1 - \frac{0.5}{0.75} \tanh \left(\frac{0.75}{0.5}\right) = 0.397 \ ,$$

$$\zeta_1 = 0.397 \times 0.734 \times 10^{-4} \left(\frac{0.5}{0.01}\right) \times 0.82 \ \frac{1.5}{(2.58 + 0.734) \times 10^{-4} \times 48 \times 12}$$

$$= 0.94\% \ .$$

Therefore, the total fluid damping is equal to

$$\zeta_1 = 0.083\% + 0.94\% = 1.02\% \ .$$

VII. CONCLUDING REMARKS

Fluid damping is important; however, its characteristics for general cases are still difficult to quantify. In particular, very few data are available for cylinder arrays. Systematic theoretical and experimental studies remain to be done in evaluating the damping matrices α_{ij}', σ_{ij}', τ_{ij}', and β_{ij}' as functions of geometry, reduced flow velocity, and flow direction as well as other system parameters.

When cylinder motion is small, a linear representation of fluid damping as given in Eq. 1 is applicable. However, when cylinder motion becomes large, other flow phenomena, such as vortex shedding, and cylinder/flow interaction, become significant; more detailed characterization of the damping effect will be needed.

At present, most of the mathematical models for cylinders vibrating in a flow are based on the damping value obtained in stationary fluid. It has been shown that flow-velocity dependent damping can be very important. Without considering the flow velocity-dependent force, we may reach erroneous conclusions.

ACKNOWLEDGMENTS

REFERENCES

1. Chen, S. S., "Fluid Damping for Circular Cylindrical Structures," Nucl. Eng. Des. 63, 81-100 (1981).

2. Chen, S. S., "Vibration of Nuclear Fuel Bundles," Nucl. Eng. Des. 35, 399-422 (1975).

3. Chen, S. S., "Crossflow-induced Vibrations of Heat Exchanger Tube Banks," Nucl. Eng. Des. 47, 67-86 (1978).

4. Chen, S. S., Wambsganss, M. W., and Jendrzejczyk, J. A., "Added Mass and Damping of a Vibrating Rod in Confined Viscous Fluids," J. Appl. Mech. 98(2), 325-329 (1976).

5. Yeh, T. T., and Chen, S. S., "The Effect of Fluid Viscosity on Coupled Tube/Fluid Vibrations," J. Sound Vibr. 59(3), 453-467 (1978).

6. Sinyavaskii, V. F., Fedotovskii, V.S., and Kukhtin, A. B., "Oscillation of a Cylinder in a Viscous Liquid," Prikladnaya Mekhanika, 16(1), 62-27 (1980).

7. Williams, R. E., and Hussey, R. G., "Oscillating Cylinders and the Stokes' Paradox," The Physics of Fluids 15(12), 2083-2088 (1972).

8. Mulcahy, T. M., "Fluid Forces on Rods Vibrating in Finite Length Annular Regions," J. Appl. Mech. 47, 234-240 (1980).

9. Yang, C. I., and Moran, T. J., "Finite-Element Solution of Added Mass and Damping of Oscillating Rods in Viscous Fluids," Technical Memorandum ANL-CT-78-22 (1978).

10. Lin, H. C., and Chen, S. S., "Acoustically Induced Vibration of Circular Cylindrical Rods," J. Sound Vibr. 51(1), 89-96 (1977).

11. Shimogo, T., Niino, T., and Setogawa, S., "Coupled Vibration of Elastic Circular Bars in Viscous Fluid," ASME Paper No. 75-DET-76 (1975).

12. Chen, S. S., Jendrzejczyk, J. A., and Wambsganss, M. W., "An Experimental and Theoretical Investigation of Coupled Vibration of Tube Banks," Fluid Structure Interaction Phenomena in Pressure Vessel and Piping Systems, ASME, 19-36 (1977).

13. Carlucci, L. N., "Damping and Hydrodynamic Mass of a Cylinder in Simulated Two-Phase Flow" ASME J. Mech. Des. 102(3), 597-602 (1980).

14. Carlucci, L. N., and Brown, L. D., " Experimental Studies of Damping and Hydrodynamic Mass of a Cylinder in Confined Two-Phase Flow," J. Vibration, Acoustics, Stress and Reliability in Design 105, 83-89 (1982).

15. Hara, F., and Kolgo, O., "Added Mass and Damping of a Vibrating Rod in a Two-Phase Air-Water Mixed Fluid," Flow-Induced Vibration of Circular Cylindrical Structures, 1982, ASME Publication PVP Vol. 63, pp 1-8 (1982).

16. Schumann, V., "Virtual Dinsity and Speed of Sound in a Fluid-Solid Mixture With Periodic Structures," Int. J. Multiphase Flow $\underline{7}$(6), 619-633 (1981).

17. Collier, J. G., "Connective Boiling and Condensation," 1st ed., McGraw Hill, London, 1972.

18. Warburton, G. B., "Vibration of a Cylindrical Shell in an Acoustic Medium," J. Mech. Eng. Sci. $\underline{3}$(1), 69-79 (1961).

19. Yeh, T. T., and Chen, S. S., "Dynamics of a Cylindrical Shell System Coupled by Viscous Fluid," J. Acoust. Soc. Am. $\underline{62}$(2), 262-270 (1977).

20. Chung, H., Turula, P., Mulcahy, T. M., and Jendrzejczyk, J. A., "Analysis of Cylindrical Shell Vibrating in a Cylindrical Fluid Region," Nucl. Eng. Des. $\underline{63}$, 109-120 (1981).

21. Chu, M. L, and Brown, J., "Experiments on the Dynamic Behavior of Fluid-Coupled Concentric Cylinders," Experimental Mechanics, 129-137 (April 1981).

22. Lin, W. H. and Chen, S. S., "On the Added Mass and Radiation Damping of Rod Bundles Oscillating in Compressible Fluids," J. Sound Vibr. $\underline{74}$(3), 441-453 (1981).

23. Varadan, V. K. and Varadan, V. V. (eds.), "Acoustic, Electromagnetic, and Elastic Wave Scattering-Focus on the T-Matrix Approach," Pergamon Press, 1980.

24. Skop, R. A., Ramberg, S. E., and Ferer, K. M., "Added Mass and Damping Forces on Circular Cylinders," ASME Paper No. 76-PET-3 (Sept. 1976).

25. Benjamin, T. B., "Dynamics of a System of Articulated Pipes Conveying Fluid: I. Theory, II. Experiment," Proc. Royal Soc. London $\underline{261}$ (Series A), 457-499 (1961).

26. Housner, G. W., "Bending Vibrations of a Pipe Line Containing Flowing Fluid," J. Appl. Mech., Trans. ASME $\underline{19}$(2), 205-208 (1952).

27. Gregory, R. W, and Paidoussis, M. P., "Unstable Oscillating of Tubular Cantilever Converging Fluid; II; Experiment," Proc. Roy. Soc. London $\underline{A293}$, 528-542 (1961).

28. Chen, S. S., "Vibration and Stability of a Uniformly Curved Tube Conveying Fluid," J. Acoust. Soc. Am. $\underline{51}$(1), 223-232 (1971).

29. Chen, S. S., "Out-of-Plane Vibration and Stability of Curved Tubes Conveying Fluid," J. Appl. Mech., Trans. ASME $\underline{95}$, 362-368 (1976).

30. Chen, S. S., "Dynamic Stability of a Tube Conveying Fluid," J. Eng. Mech. Div., Proc. ASME 97, 1469-1485 (1971).

31. Ginsberg, J. H., "The Dynamic Stability of a Pipe Conveying a Pulsating Flow," Int. J. Eng. Sci. 11, 1013-1024 (1973).

32. Paidoussis, M. P., and Issid, N. T., "Experiments on Parametric Resonance of Pipes Containing Flow," ASME, J. Appl. Mech. 43, 198-202 (1976).

33. Hara, F., "Two-Phase-Flow-Induced Vibrations in a Horizontal Piping System," Bull. JSME 20(142), 419-427 (1977).

34. Chen, S. S., and Wambsganss, M. W., "Parallel-Flow-Induced Vibration of Fuel Rods," Nucl. Eng. Des. 18, 253-278 (1972).

35. Wambsganss, M. W., and Jendrzejczyk, J. A., "The Effect of Trailing End Geometry on the Vibration of a Circular Cantilevered Rod in Nominally Axial Flow," J. Sound Vibr. 65(2), 251-258 (1979).

36. Paidoussis, M. P., and Suss, S., "Stability of a Cluster of Flexible Cylinders in Bounded Axial Flow," Trans. ASME, J. Appl. Mech. 44, 401-408 (1977).

37. Connors, H. J., Savorelli, S. J., and Kramer, F. A., "Hydrodynamic Damping of Rod Bundles in Axial Flows," Flow-Induced Vibration of Circular Cylindrical Structures," ASME PVP Vol. 63, 109-124 (1982).

38. Widnall, S. E. and Dowell, E. H., "Aerodynamic Forces on an Oscillating Cylindrical Duct with an Internal Flow," J. Sound Vibr. 6(1), 71-85 (1967).

39. Clinch, J. M., "Prediction and Measurement of the Vibrations Induced in Thin-Walled Pipes by the Passage of Internal Turbulent Water Flow," J. Sound Vibr. 12(4) 429-451 (1970).

40. Chen, S. S. and Rosenberg, G. S., "Free Vibrations of Fluid-Conveying Cylindrical Shells," Trans. ASME, J. Eng. Ind. 96, 420-426 (1974).

41. Chen, T. L. C. and Bert, C. W., "Dynamic Stability of Isotropic or Composite-Material Cylindrical Shells Containing Swirling Fluid," Trans. ASME, J. Appl. Mech. 99, 112-116 (1977).

42. Blevins, R. D., "Flow-Induced Vibration," Van Nostrand Reinhold Co., 1977.

43. Chen, S. S., and Jendrzejczyk, J. A., "Dynamic Response of a Circular Cylinder Subjected to Liquid Cross Flow," J. Press. Vessel Technol. 101, 106-112 (1979).

44. Griffin, O. M., and Koopman, G. H., "The Vortex-Excited Lift and Reaction Forces on Resonantly Vibrating Cylinders," J. Sound Vibr. 54(3), 435-448 (1977).

45. Souders, W. G., Coder, D. W., and Nelka, J. J., "Experimental Measurements of Lift and Drag on an Oscillating Smooth Circular Cylinder in Crossflow," Naval Ship Research and Development Center, Hydromechanics Laboratory Test and Evaluation Report 302-M-01 (1968).

46. Kato, M., et al., "Drag Forces on Oscillating Cylinders in Uniform Flow," presented at the 15th Annual OTC in Houston, Texas, May 2-5, 1983.

47. Zdravkovich, M. M., "Review - Review of Flow Interference Between Two Circular Cylinders in Various Arrangements," J. Fluids Eng. 94, 618-633 (1977).

48. Jendrzejczyk, J. A., Chen, S. S., and Wambsganss, M. W., "Dynamic Responses of a Pair of Circular Tubes Subjected to Liquid Cross Flow," J. Sound Vibr. 67(2), 263-273 (1979).

49. Tsui, Y. T., and Tsui, C. C., "On Wake Induced Flutter of a Circular Conductor in the Wake of Another," Flow Induced Vibration, ASME, pp. 19-33 (1979).

50. Chen, S. S., and Jendrzejczyk, J. A., "Flow-Velocity-Dependence of Damping in Tube Arrays Subjected to Liquid Cross Flow," J. Press. Vessel Technol. 103, 130-135 (1981).

51. Tanaka, H., "A Study on Fluid Elastic Vibration of a Circular Cylinder Array (One-row Cylinder Array)," Trans. Japan Soc. Mech. Eng. 46(408) (Section B), 1398-1407 (1980).

52. Tanaka, H., and Takahara, S., "Fluid Elastic Vibration of Tube Array in Cross Flow," J. Sound Vibr. 77, 19-37 (1981).

53. Tanaka, M., Takahara, S., and Ohta, K., "Flow-Induced Vibration of Tube Arrays with Various Pitch-to-Diameter Ratios," Flow-Induced Vibration of Circular Cylindrical Structures, ASME, pp. 45-56 (1982).